Computational Method to Perform the Flaw Evaluation Procedure as Specified in the ASME Code, Section XI, Appendix A Part 1: General Description and Background

NP-1181 MASTER
Research Project 700-1

Key Phase Report, September 1979

Prepared by

FAILURE ANALYSIS ASSOCIATES 750 Welch Road, Suite 116 Palo Alto, California 94304

Principal Investigator R. C. Cipolla

Prepared for

Electric Power Research Institute 3412 Hillview Avenue Palo Alto, California 94304

> EPRI Project Manager F. E. Gelhaus Nuclear Power Division

DISCLAIMER

This report was prepared as an account of work sponsored by an agency of the United States Government. Neither the United States Government nor any agency thereof, nor any of their employees, makes any warranty, express or implied, or assumes any legal liability or responsibility for the accuracy, completeness, or usefulness of any information, apparatus, product, or process disclosed, or represents that its use would not infringe privately owned rights. Reference herein to any specific commercial product, process, or service by trade name, trademark, manufacturer, or otherwise does not necessarily constitute or imply its endorsement, recommendation, or favoring by the United States Government or any agency thereof. The views and opinions of authors expressed herein do not necessarily state or reflect those of the United States Government or any agency thereof.

DISCLAIMER

Portions of this document may be illegible in electronic image products. Images are produced from the best available original document.

ORDERING INFORMATION

Requests for copies of this report should be directed to Research Reports Center (RRC), Box 50490, Palo Alto, CA 94303, (415) 961-9043. There is no charge for reports requested by EPRI member utilities and affiliates, contributing nonmembers, U.S. utility associations, U.S. government agencies (federal, state, and local), media, and foreign organizations with which EPRI has an information exchange agreement. On request, RRC will send a catalog of EPRI reports.

Copyright © 1979 Electric Power Resourch Institute, Ins

EPRI authorizes the reproduction and distribution of all or any portion of this report and the preparation of any derivative work based on this report, in each case on the condition that any such reproduction, distribution, and preparation shall acknowledge this report and EPRI as the source.

NOTICE

This report was prepared by the organization(s) named below as an account of work sponsored by the Electric Power Research Institute, Inc. (EPRI). Neither EPRI, members of EPRI, the organization(s) named below, nor any person acting on their behalf: (a) makes any warranty or representation, express or implied, with respect to the accuracy, completeness, or usefulness of the information contained in this report, or that the use of any information, apparatus, method, or process disclosed in this report may not infringe privately owned rights; or (b) assumes any liabilities with respect to the use of, or for damages resulting from the use of, any information, apparatus, method, or process disclosed in this report.

Prepared by Failure Analysis Associates Palo Alto, California

EPRI PERSPECTIVE

PROJECT DESCRIPTION

One area addressed by the Nuclear Power Division's program on Reliability, Availability, and Economics of Light Water Reactors is the structural integrity of major components. One of the most important components is the reactor pressure vessel that contains the reactor fuel and cooling water. The American Society of Mechanical Engineers (ASME) develops criteria for acceptable structural integrity of all pressure vessels. The Code of Federal Regulations requires all nuclear reactor vessels to meet the ASME criteria. Occasionally, a nondestructive examination identifies a flaw in a reactor pressure vessel. The ASME Boiler and Pressure Vessel code, Section XI, Appendix A, provides a procedure for evaluating such a flaw. The procedure is used to determine whether the flaw must be repaired.

PROJECT OBJECTIVE

The ASME flaw evaluation procedure is quite time-consuming because it involves interpolation of graphs and evaluation of equations. The purpose of this phase of the project is to automate the evaluation procedure so that flaws can be evaluated quickly.

PROJECT RESULTS

The FACET computer program described in this key phase report provides a tool for performing the ASME flaw evaluation procedure. It can be applied directly by pressure vessel manufacturers, owners, and inspectors. Similar proprietary computer programs have been written by others; FACET can also be used as an independent check of those programs.

Floyd Gelhaus, Project Manager Nuclear Power Division

		The first of the second of the second section is a second of the second	and the second of the second o	
				•
•				

ABSTRACT

The fracture mechanics procedures required to evaluate indications found during in-service inspection of reactor pressure vessels are specified in the ASME Boiler and Pressure Vessel Code, Section XI. This report describes the computer program, FACET, which performs quickly and accurately the flaw evaluation specified in Appendix A of Section XI. Specifically, FACET determines the crack-tip stress intensity factor range, the corresponding crack growth and whether the maximum crack size that could develop during the remaining service life approaches the minimum crack size allowable. FACET is written in FORTRAN and presently runs on an IBM 370/168 computer. Various input and output options are available; FACET can utilize either actual materials data or the conservative estimates which are provided in Section XI.

	•

ACKNOWLEDGMENTS

The author gratefully acknowledges Mr. Phil Besuner, who provided technical and editorial comments and Mr. John Rice who assisted in the numerical analysis development. Also, the author acknowledges Dr. Sumio Yukawa of General Electric and Dr. Spencer Bush of Battelle Northwest for providing details regarding the background and basis of the Code procedure. The Electric Power Research Institute is gratefully acknowledged for financial support under contracts RP 217-1 and RP 700-1.

		The second of th	
			•
			•

NOMENCLATURE

SYMBOL	DEFINITION
a	Crack depth
a a	Crack depth at crack arrest
^a c	Minimum critical flaw for normal, upset, and test conditions
a _f	Maximum expected flaw size for the remaining life of the component
a _i	Minimum critical crack size for initiation of unstable fracture for emergency and faulted conditions
^a o	Original or initial crack depth
^a tol	Tolerance limit on crack depth in convergence criteria
a/ /	Crack depth-to-length aspect ratio
С	Coefficient in fatigue crack growth relations
da/dN	Crack growth rate on a cyclic basis
Ε	Fast neutron energy fluence
e	Flaw eccentricity relative to the section centerline
K	Stress intensity factor usually referring to $K_{\overline{\mathbf{I}}}$
ĸ _I	Stress intensity factor for Mode I loading
K _{Ia}	Arrest fracture toughness (plane strain)

NOMENCLATURE (Continued)

<u>SYMBOL</u>	DEFINITION
K _{Ic}	Static fracture toughness (plane strain)
K _{max}	Maximum applied $K_{\overline{I}}$ in the stress cycle
K _{mean}	Mean K_{I} level in the stress cycle
K _{min}	Minimum applied $K_{\overline{I}}$ in the stress cycle
ΔK_{I}	Range of applied $K_{\overline{I}}$ in the stress cycle
l	Crack length
М _b	Free-surface K correction factor for bending loads
M _m	Free-surface K correction factor for membrane loads
n	Exponent in fatigue crack growth rate relations
N	Number of applied cycles
NDT	Nil ductility temperature
N _{to1}	Tolerance limit on cycles in convergence criteria
р	Crack penetration (a/t for surface flaws and $2a/t$ for subsurface flaws)
Q	Flaw shape parameter
R	Ratio of K _{min} to K _{max}
RT _{NDT}	Reference nil ductility temperature

NOMENCLATURE (Continued)

SYMBOL	DEFINITION
∆RT _{NDT}	Change in RT _{NDT} due to irradiation
σ	Applied stress
σ(x)	Univariate stress distribution
σ̂(x)	Equivalent Linear Representation of $\sigma(x)$
$^{\sigma}_{b}$	Applied bending stress
σ_{m}	Applied uniform stress
σ _{max}	Maximum applied stress in cycle
σ _{min}	Minimum applied stress in cycle
σ _y	Material yield strength
Δσ	Cyclic stress range
T(x)	Univariate temperature distribution
t	Wall thickness
x	Global x coordinate
×c	Global x coordinate for crack center

				•
				,
		•		

CONTENTS

SECTION	TITLE	PAGE NUMBER
1.0 1.1 1.2 1.3	INTRODUCTION Background Scope Program Documentation	1-1 1-1 1-2 1-3
2.0 2.1 2.2 2.3	SECTION XI FLAW EVALUATION PROCEDURE Introduction Linear Elastic Fracture Mechanics Concepts Section XI Evaluation Procedure and the FACET	2-1 2-1 2-1 2-4
2.4 2.5 2.6	Program Elliptical Flaw Model Definition of Material Properties and Require- ments for Testing Stress Analysis	2-7 2-7 2-13
3.0 3.1 3.2 3.3 3.4 3.5 3.5.1 3.5.2 3.5.3	PROGRAM DESCRIPTION General Description Representation of the Applied Stresses Calculation of the Stress Intensity Factor, K _I Selection of Material Properties Method of Analysis Determination of End-of-Life Flaw Size (a _f) Determination of Minimum Critical Flaw Size for Initiation (a _i)	3-1 3-1 3-1 3-3 3-4 3-10 3-10 3-12 3-15
4.0 4.1 4.2 4.3	PROGRAM CAPABILITIES AND RESTRICTIONS Data Input Description Problem Execution and Output Problem Size Limits	4-1 4-1 4-3 4-4
5.0	SIMPLE EXAMPLE PROBLEM	5-1
6.0	SUMMARY AND CONCLUSIONS	6-1
7.0	REFERENCES	7-1
APPENDIX A	EQUATIONS TO COMPUTE K, USING	A-1

		•	-
			٠
•			

ILLUSTRATIONS

Figu	<u>re</u>	Page
2.1	Review of Linear Elastic Fracture Mechanics.	2-3
2.2	Functional Diagram Showing ASME Section XI Flaw Evaluation Procedure.	2-5
2.3	Flaw Model Geometry for Surface and Sub-Surface Flaws.	2-8
2.4	Lower Bound Toughness Curves From Tests of SA-533B-1, SA-508-2, and SA-508-3 Steel (Section XI, Fig. A-4200-1).	2-10
2.5	Effect of Fast Neutron Fluence and Copper Content on Shift of RT_{NDT} for Reactor Vessel Irradiation at 550 F (Section XI, Fig. A-4400-1).	2-11
2.6	Upper Bound Fatigue Crack Growth Data for Reactor Vessel Steels (Section XI, Fig. A-4300-1).	2-12
3.1	Linearized Representation of Stresses (Section XI, Fig. A-3200-1).	3-2
3.2	Shape Factor for Flaw Model (Section XI, Fig. A-3000-1).	3-5
3.3	Membrane Correction Factor for Sub-Surface Flaws (Section XI, Fig. A-3300-2).	3-6
3.4	Membrane Correction Factor for Surface Flaws (Section XI, Fig. 3300-3).	3-7
3.5	Bending Correction Factor for Surface Flaws (Section XI, Fig. A-3300-4).	3-8
3.6	Bending Correction Factor for Surface Flaws (Section XI, Fig. A-3300-5).	3-9
3.7	Determination of a Critical Flaw Size, a _c , for Normal Conditions.	3-14
3.8	Determination of Critical Flaw Sizes for Postulated Conditions (Section XI, Fig. A-5300-1).	3-17
5.1	Calculated Stress Intensity Factor Versus Crack Depth.	5-2
5.2	Calculated Crack Depth Versus Applied Cycles.	5-3

	en e	
		•
		•
	•	

xvii

TABLES

<u>Table</u>		Page
4.1	Card Input Description for FACET.	4-2
4.2	Present Limits on Problem Size in FACET.	4-5

SUMMARY

The nuclear power industry has utilized thorough inspection and testing of components during manufacture, construction, and initial start-up phase. However, the industry also recognizes the need for a continuing in-service inspection program. In 1969, the idea for on-going surveillance was put into practice with the Atomic Energy Commission announced licensing regulations that included in-service inspection. Soon after, Section XI of the ASME Boiler and Pressure Vessel Code (BPVC) appeared as the first mandatory in-service inspection procedure for nuclear plant components.

The purpose of Section XI is to assure the mechanical integrity of the pressure boundary of a plant for its expected service life. Prior to the introduction of an evaluation technique into Section XI, the only action possible if imperfections were discovered during service was to repair or replace the component. In the case of welded pressure vessels, however, either repair or replacement are difficult for both economic and technical reasons. Changes and additions to Section XI now provide for a conservative flaw evaluation procedure based on the principles of fracture mechanics. Flaws that exceed the inspection standards can be analytically evaluated to determine if the imperfection detected during service could grow to a dangerous size during the remaining service life of the component. Upon satisfying the flaw acceptibility criteria, and subject to approval by the regulatory authority, a component may be returned to service without repair.

The Flaw Analysis and Code Evaluation Technique (FACET) is a computerized tool which performs the evaluation procedure specified in Appendix A of Section XI. Specifically, FACET determines the crack-tip stress intensity

factor range, the corresponding crack growth, and whether the maximum crack size that could develop during the remaining service life approaches the minimum crack size allowable. The purpose of FACET is three-fold. First, it provides a tool which can be rapidly and accurately applied to evaluate flaw indications. Secondly, FACET can be used to analyze hypothetical flaws to investigate the flaw behavior under various or parametric conditions (e.g., to determine whether the end-of-life flaw is acceptable based on the applicable criteria of Paragraph IWB-3600 of Section XI). Finally, through applications of FACET described previously, areas where the Section XI procedure might be expanded or improved can be identified. Thus, FACET can serve as a tool for both performing Section XI analyses and improving the methodology. There are other computer codes developed by certain vendors, which perform similar computations, but these are proprietary programs and are, in general, unavailable to the industry.

FACET is a modular computer program written in FORTRAN and is comprised of a main program with a series of subroutines and function routines. FACET is a relatively small program using approximately 130K bytes memory, all array addressing is performed in core. The program was developed for an IBM 370/168 computing system, with some variables being declared as double precision. Various input and output options are available, and FACET can utilize either actual materials data or the conservative estimates which are provided in Section XI.

The documentation of FACET is in three parts. This report (Part I) gives the background and general description of the FACET program, including its capabilities and restrictions. The details of problem definition and program use are described in Part II, the User's Manual. Also contained in

Part II is the definition of the input parameters, the input card description, and sample problems. Part III is the Programmer's Guide to FACET which provides the details of the program logic, subroutine functions, and a program source listing. All documents and the program source code are available through the Electric Power Research Institute's Electric Power Software Center, managed by Technology Development Corporation, 155 Moffett Park Drive, Building C, Sunnyvale, California 94086.

1.0 INTRODUCTION

1.1 Background

The nuclear power industry has utilized thorough inspection and testing of components during manufacture, construction, and initial start-up phase. However, the industry also recognizes the need for a continuing in-service inspection program. In 1969, the idea for on-going surveillance was put into practice when the Atomic Energy Commission (AEC) announced licensing regulations that included in-service inspection. Soon after, Section XI of the ASME Boiler and Pressure Vessel Code (BPVC) (1-1) appeared as the first mandatory in-service inspection procedure for nuclear plant components.

The purpose of Section XI is to assure the mechanical integrity of the pressure boundary of a plant for its expected service life. Prior to the introduction of an evaluation technique into Section XI, the only action possible if imperfections were discovered during service was to repair or replace the component. In the case of welded pressure vessels, however, either repair or replacement are difficult for both economic and technical reasons. Because the in-service inspection requirements of Section XI are different than the pre-service requirements of Section III of the ASME BPVC, inspection indications were recorded during the extensive baseline ultrasonic examination required by Section XI in an actual pressure vessel subsequent to being Code-stamped in 1971. The locations and orientation of the flaws were such to make detectability very difficult. The need to reassess the adequacy of Section XI was apparent and several major changes were introduced.

Specifically, changes and additions to Section XI now provide for a conservative flaw evaluation procedure based on the principles of fracture mechanics. Flaws that exceed the inspection standards can be analytically evaluated to determine if the imperfection detected during service could grow to a dangerous size during the remaining service life of the component. Upon satisfying the flaw acceptibility criteria, and subject to approval by the regulatory authority, a component may be returned to service without repair.

1.2 Scope

The fracture mechanics evaluation procedures are specified in Appendix A of Section XI where the details regarding the fatigue and static overload calculations and the required flaw size limits are presented. The Flaw Analysis and Code Evaluation Technique (FACET) is a computerized tool which performs the evaluation procedure specified in Appendix A of Section XI. The purpose of FACET is three-fold. First, it provides a tool which can be rapidly and accurately applied to evaluate actual flaw indications. Secondly, FACET can be used to analyze hypothetical flaws to investigate the flaw behavior under various or parametric conditions (e.g., to determine whether the end-of-life flaw is acceptable based on the applicable criteria of Paragraph IWB-3600 of Section XI). Finally, through applications of FACET described previously, areas where the Section XI* procedure might be expanded or improved can be identified. Thus, FACET can serve as a tool for both performing Section XI analyses and improving the methodology. There are other computer programs developed by certain manufacturers, such as (1-2),

^{*}Further referral to "Section XI" will mean Appendix A of Section XI of the ASME Boiler and Pressure Vessel Code (1-1), unless otherwise qualified.

which perform similar computations, but these are proprietary programs and are, in general, unavailable to the industry.

1.3 Program Documentation

The documentation of FACET is in three parts. This report (Part I) gives the background (Section 2.0) and general description (Section 3.0) of the FACET program, including its capabilities and restrictions (Section 4.0). The details of problem definition and program use are described in Part II, the User's Manual (1-3). Also contained in Part II is the definition of the input parameters, the input card description, and sample problems. Part III is the Programmer's Guide to FACET which provides the details of the program logic, subroutine functions, and a program source listing (1-4). All documents and the program source code are available through the Electric Power Research Institute's Electric Power Software Center, managed by Technology Development Corporation, 155 Moffett Park Drive, Building C, Sunnyvale, California 94086.

REFERENCES

- 1-1 ASME Boiler and Pressure Vessel Code, Section XI, "Rules for In-Service Inspection of Nuclear Power Plant Components," 1977 Edition, Summer 1977 Addenda.
- Ayres, D. J. "Section XI, A Computer Program for the Evaluation of Flaw Indications According to ASME Boiler and Pressure Vessel Code, Sections XI, Appendix A," Combustion Engineering Document ESD-74-43.
- 1-3 Cipolla, R. C. "Computational Method to Perform the Flaw Evaluation Procedure as Specified in the ASME Code, Section XI, Appendix A, Part II: User's Manual," EPRI RP700-1, Technical Report (to be published).
- 1-4 Cipolla, R. C. "Computational Method to Perform the Flaw Evaluation Procedure as Specified in the ASME Code, Section XI, Appendix A, Part III: Programmer's Manual," EPRI RP700-1, Technical Report (to be published)

2.0 SECTION XI FLAW EVALUATION PROCEDURE

2.1 <u>Introduction</u>

The flaw evaluation procedure for determining the acceptability of flaws that exceed the allowable flaw indication standards of Paragraph IWB-3500 is contained in Appendix A of Section XI. Appendix A is considered non-mandatory in that the evaluation of detected flaws need not be performed if repair is made. The procedures are intended for structures of thickness four inches or greater, made of ferritic materials with specified minimum yield strengths of 50 ksi or less, and with simple geometries and stress distributions. The analytical techniques specified are only recommendations rather than requirements and may be inadequate in some cases. Furthermore, according to the Section XI, alternative techniques may be used and the analysis may be extended to other materials, more complex geometries, and stress states so long as the alternative methods and analyses used are documented and shown to be adequate. One possible alternative technique which provides analytical refinements for computing the stress intensity factor, K, is presented in (2-1).

2.2 Linear Elastic Fracture Mechanics Concepts

The flaw evaluation is based upon the principles of linear elastic fracture mechanics. The fracture mechanics equations effectively link three parameters: the defect size, the fracture toughness or fatigue crack growth rate of the material, and the applied stress, so that if any two of these are known, the third can be quantified. Using these principles, the Section XI

procedure assesses two potential failure events. The first is unstable extension of the flaw causing brittle fracture. The second is the subcritical propagation of the indication (flaw) which can occur in a stable manner under cyclic loading caused by transient operating conditions. This fatigue mode can continue to a point where the combination of applied stress and physical crack size causes unstable fracture.

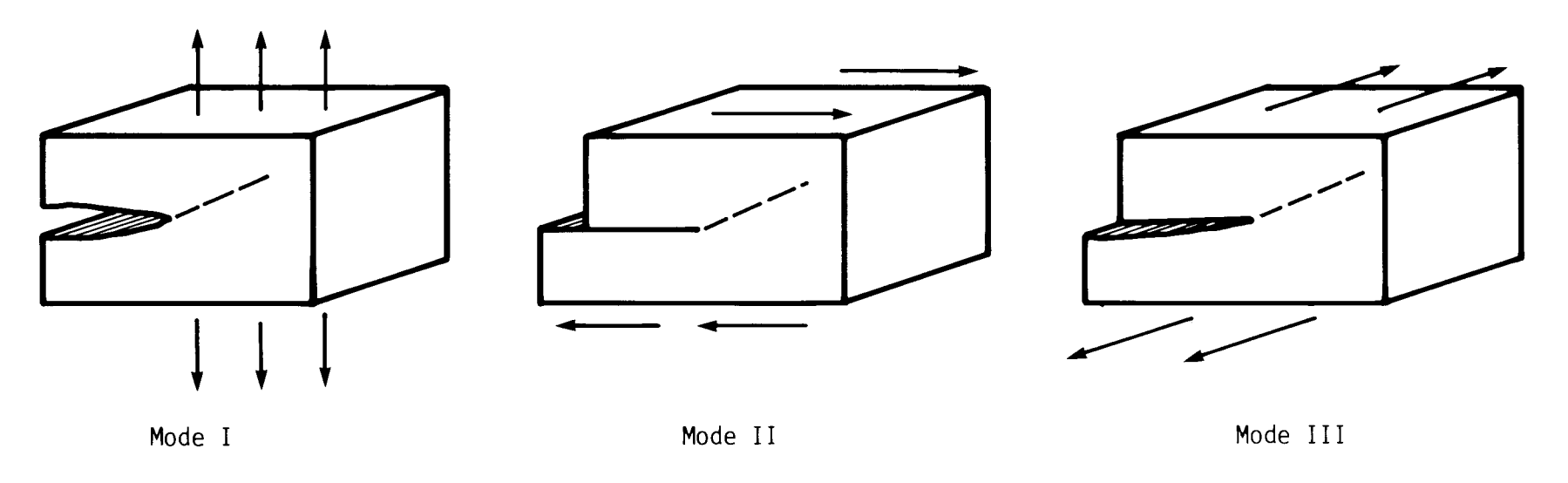
The stress distribution of a cracked structure for an arbitrary mode of loading and shape of body and crack can be quite difficult to determine. However, near the tip of the crack essentially only three things can occur: the faces can be pulled apart (Mode I) or sheared perpendicular or parallel to the leading edge of the crack (Modes II or III). These three loading modes are shown schematically in Fig. 2.1a. The crack opening mode or Mode I, in which the load is applied normal to the crack face, is normally the most damaging of the three modes. The character of the near-crack tip stress distribution is illustrated in Fig. 2.1b. The stress intensity factor, K, defines the magnitude of stress distribution and is calculated in terms of the applied, nominally uniform stress, σ , the crack length, a, and a factor that depends on the flaw geometry, stress gradients, and structural displacement constraints, F(a), from the relation

$$K = \sigma F \sqrt{\pi a}, \qquad (\sigma < \sigma_y), \qquad (2.1)$$

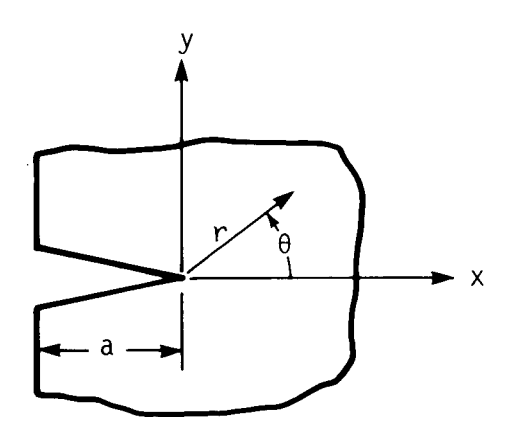
When the value of K reaches a critical value, $K_{\rm C}$, fracture will occur in an unstable manner. Thus, the critical flaw size, $a_{\rm C}$, can be determined by rearranging Eq. (2.1) to yield

$$a_c = \frac{1}{\pi} \left(\frac{K_c}{\sigma F}\right)^2$$
, (2.2)

which may be solved implicitly to evaluate a_c .



a) Crack Tip Loading Modes



All Stress Components Have the Form:

$$\sigma_{ij} = \frac{K_k}{\sqrt{2\pi r}} f_{ij}^{(k)}(\theta)$$

Where i = x, y, z; j = x, y, z, and k = I, III, III.

No Summation is Implied and Stress Intensity Factor, K is Proportional to $\label{eq:continuous} % \begin{array}{c} \text{No Summation is Implied and Stress Intensity} \\ \text{Factor}, \end{array}$

(Nominal Stress) √(Crack Length).

b) Near-Crack Tip Stress Component

Figure 2.1 - Review of Linear Elastic Fracture Mechanics.

For the assessment of a fatigue failure mode, the Section XI procedure assumes that the flaw of present size, a_0 , will grow to some final size, a_f , under the action of cyclic loading during the lifetime of the structure. If a_f exceeds a_c , the analysis predicts a brittle fracture event. Crack growth rate can be predicted from the stress intensity factor (2-2) for a given load cycle in the form of

$$da/dN = f(K), (2.3)$$

where N is the number of loading cycles. The final flaw size, $a_{\rm f}$, can be determined by integrating Eq. (2.3) using the appropriate stress distribution to calculate K, and the number of total cycles N. Values of $a_{\rm f}$ can be compared with the critical flaw size determined by Eq. (2.2) to determine if unstable fracture can occur.

2.3 Section XI Evaluation Procedure and the FACET Program

The complete evaluation procedure is described in Article A-5000 of Section XI. Figure 2.2 outlines the major steps which are to be followed with appropriate references to the governing Section XI articles. The first three blocks shown in Fig. 2.2 are tasks which must be performed before using the FACET program. Results from these three steps are used as input to FACET. The last four steps are functions which are performed by FACET. Once the flaw model has been determined and the uncracked stress distribution in the region of the crack plane is computed, the FACET code can then be utilized to determine the following critical flaw parameters.

a_f - The maximum size to which the observed flaw can grow during the remaining service lifetime of the component

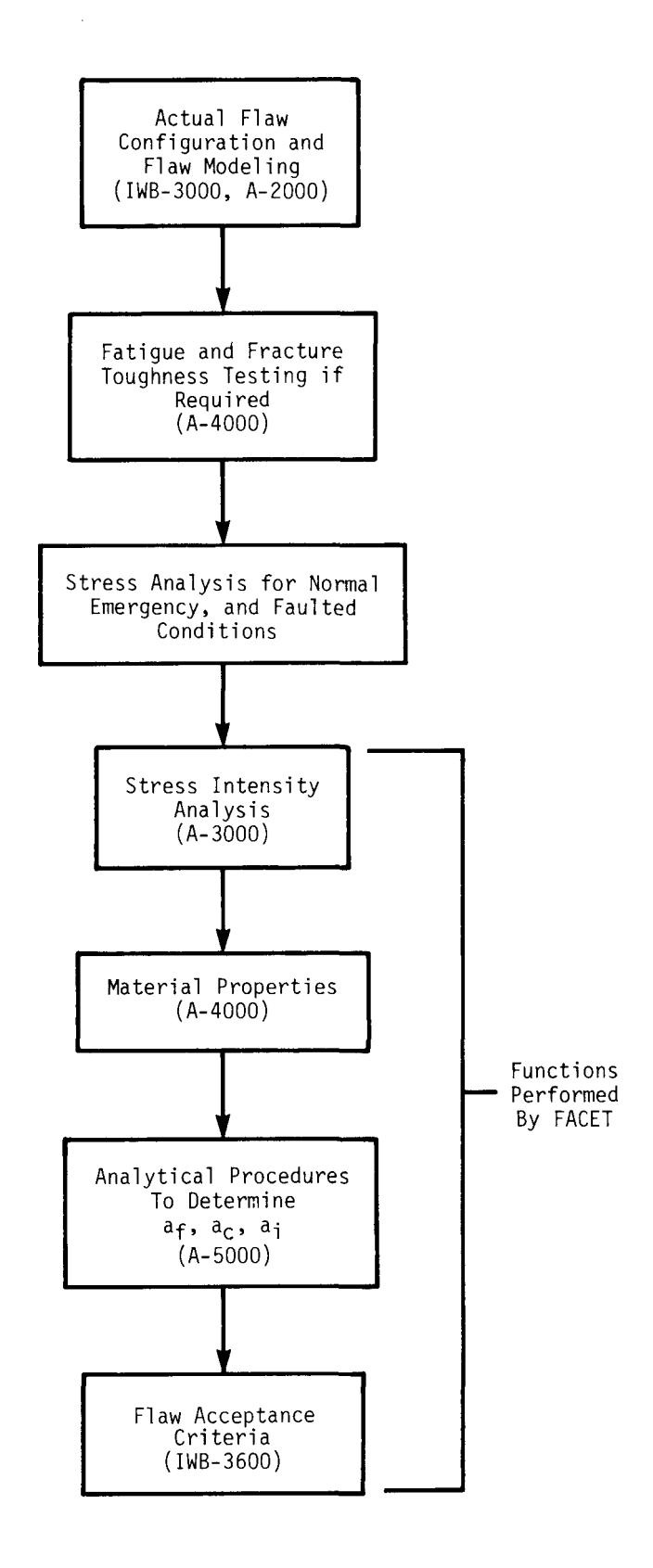


Figure 2.2 - Functional Diagram Showing ASME Section XI Flaw Evaluation Procedure.

- a_C The minimum critical size of the observed flaw under normal conditions
- ${\bf a_i}$ The minimum critical size for initiation of non-arresting growth (fast fracture) of the observed flaw under emergency and faulted conditions

The flaw acceptance criteria of Paragraph IWB-3600 require that repair may be avoided only if the following margins exist

$$a_{f} < 0.1 a_{C},$$
 (2.4)

$$a_{f} < 0.5 \ a_{j}.$$
 (2.5)

Simply stated, the above criterion (IWB-3611) requires that the computed final flaw size would have to be less than one-tenth of computed critical size for normal conditions and one-half the critical flaw size for emergency and faulted conditions. The former criteria, Eq. (2.4), can be technically unsatisfying since it imposes a severe geometric limitation for thinner vessels where ten times $\mathbf{a}_{\mathbf{f}}$ can be greater than the wall thicknesses. For this reason, an alternative criterion (IWB-3612) has been established based on stress intensity (or load) rather than crack size (2-3):

$$K_{I}(a_{f}) < K_{Ia}/\sqrt{10},$$
 (2.6)

$$K_{I}(a_{f}) < K_{Ic}/\sqrt{2}.$$
 (2.7)

The material property \mathbf{K}_{Ia} is the crack arrest toughness which is described in Section 2.5.

A more detailed discussion of the Section XI procedure to calculate stress intensity and the individual steps required to compute a_f , a_c , and a_i

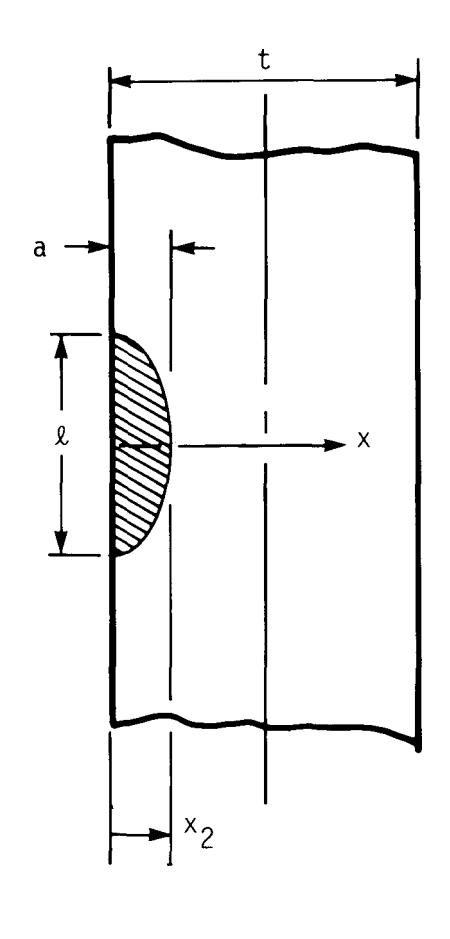
follow in Section 3.0 where the functions of the FACET program will be described. The necessary analytical steps which must be completed prior to using FACET are described next.

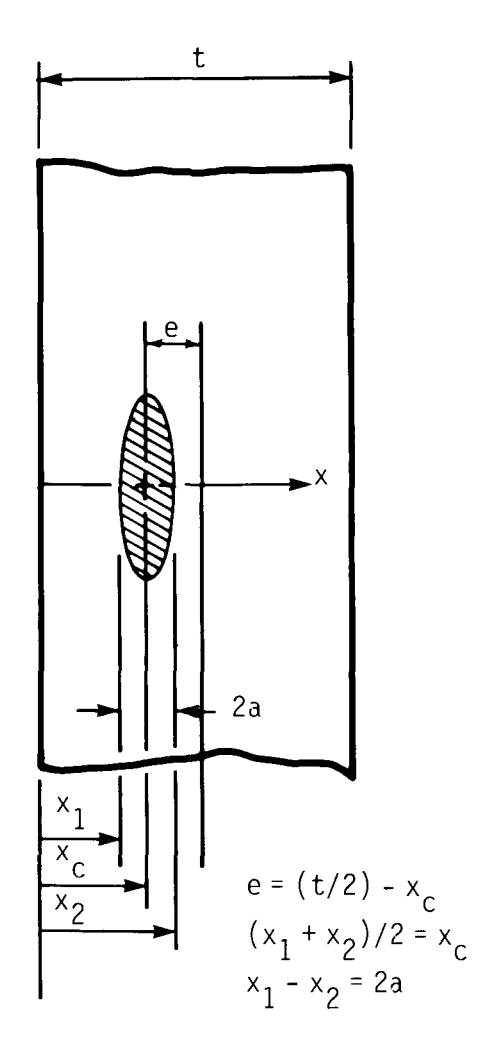
2.4 <u>Elliptical Flaw Model</u>

Flaw modeling procedures are covered in Article A-2000 and IWB-3300 in Section XI. These procedures define the size of the analytical flaw model that must be assumed, given the in-service inspection data. Both surface and subsurface indications are modeled as a flat planar discontinuity with an elliptical crack front shape. Figure 2.3 shows the geometry of these two flaw models. The elliptically-shaped crack dimensions, a and ℓ are selected to be the minimum values necessary to circumscribe the planar projection of the volume of the NDI indication. The major axis of the ellipse is parallel to the inner (pressure retaining) surface of the component and the projected planar area is considered as oriented normal to the surface of the component and to the maximum principal stress. Flaws which are initially non-planar or whose plane does not align perpendicular to the maximum principal stress directions are projected so as to obtain a projected flaw model solely under Mode I pressure loading.

2.5 Definition of Material Properties and Requirements for Testing

Definition of fracture toughness properties and fatigue crack growth rate data and the guidelines for materials testing are given in Article A-4000. Section XI defines two temperature-dependent fracture toughness properties, K_{Ic} and K_{Ia} . K_{Ic} is based on the lower bound of static initiation critical K_{I} values measured from specimens tested at several temperatures. Similarly, K_{Ia} is based on the lower bound of crack-arrest toughness data.





- a) Surface Flaws $(x_1 = 0)$
- b) Sub-Surface Flaws

Figure 2.3 - Flaw Model Geometry for Surface and Sub-Surface Flaws.

Both $\rm K_{Ic}$ and $\rm K_{Ia}$ values used in the analysis should be conservative and obtained preferably from tests using the specific material and product form analyzed. For materials that are subjected to fast neutron fluence, the degradation of material fracture toughness due to irradiation must also be accounted for in the tests. If actual data are available, lower bound $\rm K_{Ic}$ and $\rm K_{Ia}$ versus temperature curves from tests of SA-533B-1, SA-508-2, and SA-508-3 steels (2-4) are provided in Section XI and reported in Fig. 2.4. The neutron irradiation effects on material toughness can be accommodated for by shifting the transition temperature (RT $_{\rm NDT}$) as a function of irradiation using the Section XI trend curves (Fig. 2.5) for reactor vessel steels at 550F.

The fatigue crack growth rate (da/dN) of the material can be characterized by a Paris relation (2-2) in terms of the range of applied stress intensity factor ($\Delta K_{\rm I} = K_{\rm max} - K_{\rm min}$) as

$$\frac{da}{dN} = C_0 \Delta K_I^n, \qquad (2.8)$$

where n is the slope of the log (da/dN) versus log ($\Delta K_{\rm I}$) curve, and $C_{\rm O}$ is a scaling constant. The values for $C_{\rm O}$ and n, although nearly independent of stress magnitude and geometry, should be computed from test data acquired from experiments involving actual material, taking into account material variability, environment, cyclic loading frequency mean stress effects, and other important variables. If such data are unavailable, an upper bound curve for fatigue crack growth measured on SA-533B-1 and SA-508 steels which include the effects of temperature, frequency, and pressurized water environment, is provided in Section XI and shown in Fig. 2.6.

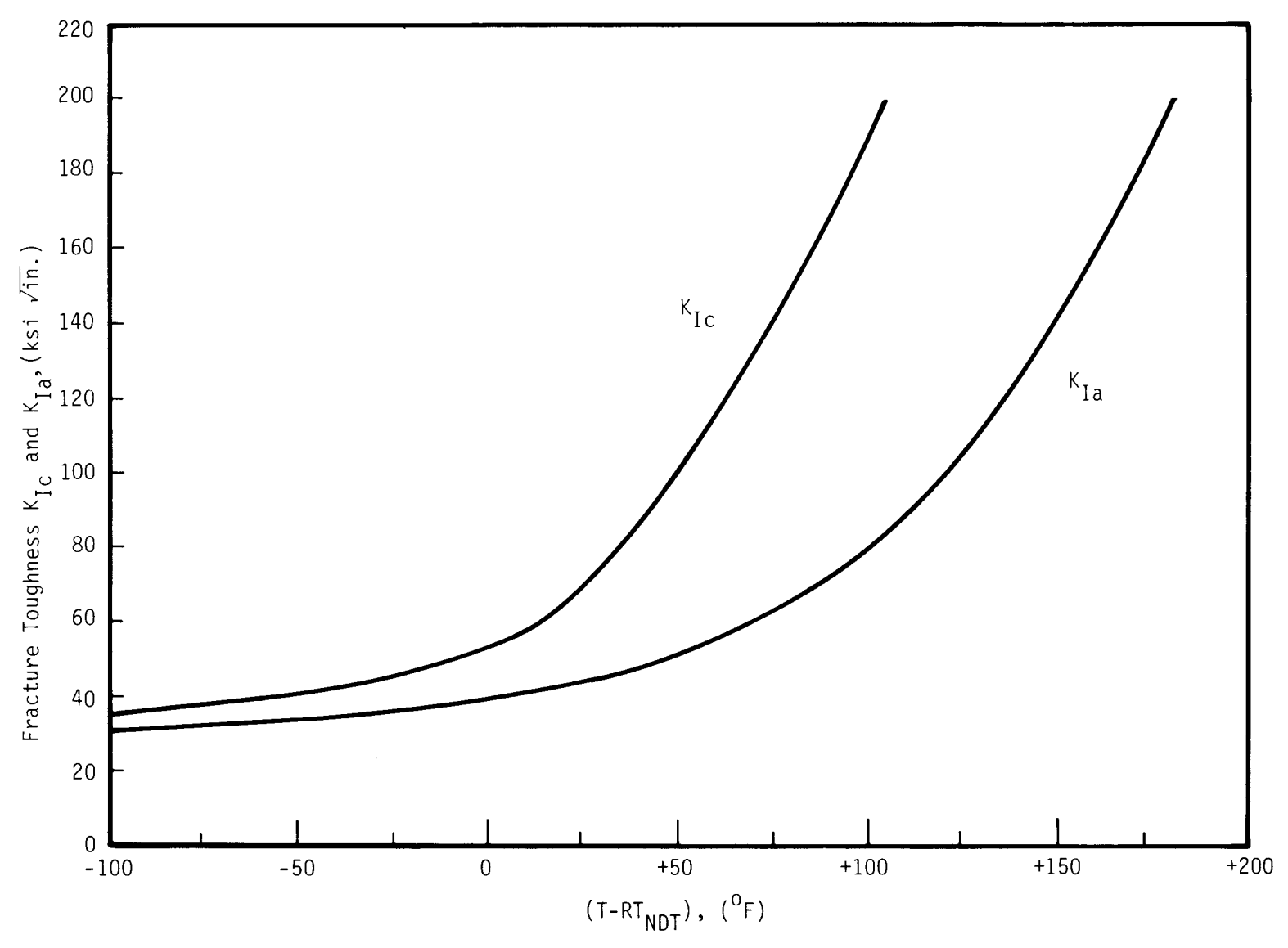


Figure 2.4 - Lower Bound Toughness Curves From Tests of SA-533B-1, SA-508-2, and SA-508-3 Steel (Section XI, Fig. A-4200-1).

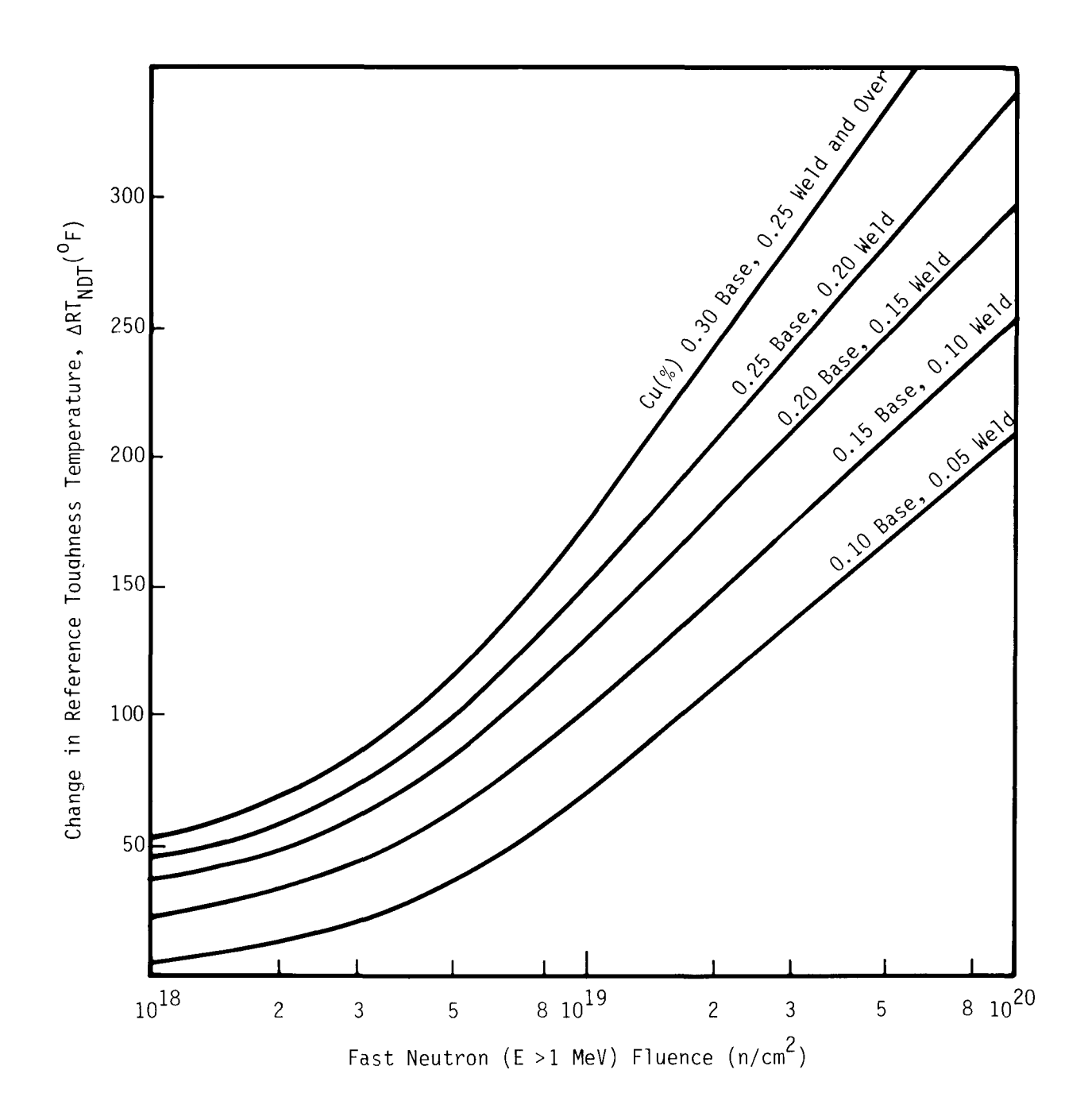


Figure 2.5 - Effect of Fast Neutron Fluence and Copper Content on Shift of RT_{NDT} FOR Reactor Vessel Irradiation at 550° F. (Section XI, Fig. A-4400-1)

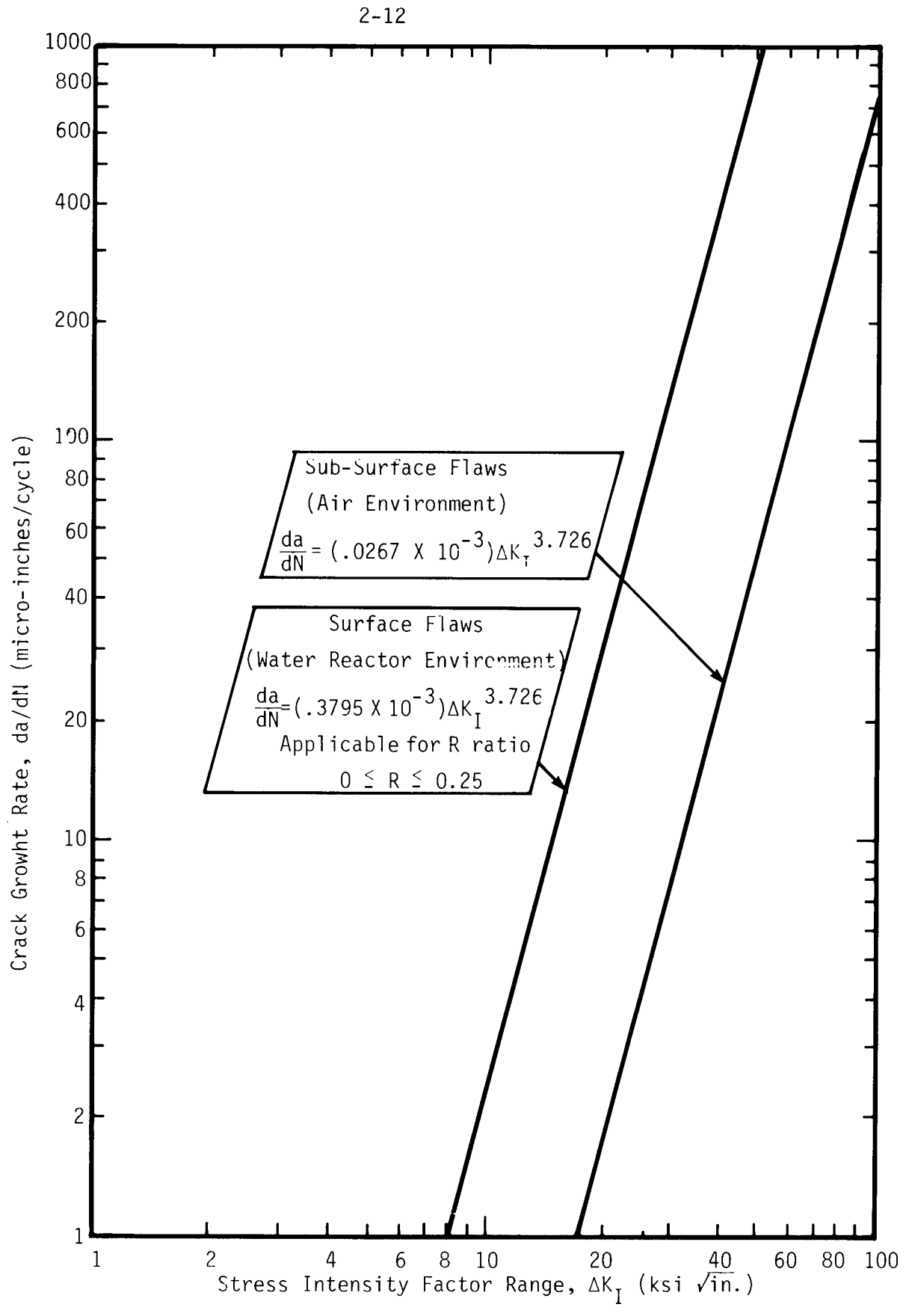


Figure 2.6 - Upper Bound Fatigue Grack Growth Data for Reactor Vessel Steels (Section XI, Fig. A-4300-1).

2.6 Stress Analysis

The variation of "uncracked" stress in the neighborhood of the flaw location must be determined for the normal, emergency, and faulted transient conditions. In determining these stress states, all forms of loading are considered including pressure, thermal, discontinuity, and residual stresses. For fracture mechanics analyses, it is important to calculate the stress in fine enough detail as to determine the through-wall distribution. For this reason, the stress analysis completed during the design of the component in order to meet Section III (2-5) requirements may be inadequate, and, in such instances, a more detailed stress analysis will have to be performed to conduct the flaw evaluation.

REFERENCES

- 2-1 Besuner, P. M., D. C. Peters, and R. C. Cipolla. "BIGIF: Fracture Mechanics Code for Structures (Introduction and Theoretical Background; Manual 1 of 3)," EPRI RP700-1, NP-838 (July 1978).
- 2-2 Paris, P. C., M. P. Gomez, and W. E. Anderson. "A Rational Analytic Theory of Fatigue," <u>The Trend in Engineering</u>, Vol 13, No 1 (January 1961).
- 2-3 ASME letter dated June 11, 1974 (ASME File #BC-74-188).
- 2-4 "PVRC Recommendations on Toughness Requirements for Ferritic Materials," Welding Research Council Bulletin, No 175 (August 1972).
- 2-5 ASME Boiler and Pressure Vessel Code, Section III, "Nuclear Power Plant Components," 1977 Edition, Summer 1977 Addenda.

3.0 PROGRAM DESCRIPTION

3.1 General Description

The FACET computer program is a modular code written in FORTRAN and is comprised of a main program with a series of subroutines and function routines. FACET is a relatively small program using approximately 130K bytes memory, and all array addressing is performed in core. The program was developed for an IBM 370/168 computing system with some variables declared as double precision.

3.2 Representation of the Applied Stresses

Under the present Section XI procedure, the stress intensity factor is evaluated from two stress states: uniform pressure or membrane stress (σ_m) and linearly varying pressure or bending stress (σ_b) . For the case when the variation of stress through the component wall is nonlinear, Section XI provides a procedure to linearize (approximate) the actual stress distribution, so that effective values of σ_m and σ_b can be defined. This technique is illustrated in Fig. 3.1 for both surface and sub-surface flaws. For the geometry shown in Fig. 3.1, one can write the equivalent linearized stress distribution $\hat{\sigma}(x)$, in terms of the actual distribution $\sigma(x)$, and crack front positions x_1 and x_2 as

$$\hat{\sigma}(x) = \frac{\sigma(x_2) - \sigma(x_1)}{(x_2 - x_1)} x + \hat{\sigma}(0). \tag{3.1}$$

For the case of surface flaws (Fig. 2.3a), $x_1 = 0$, $x_2 = a$, and $\hat{\sigma}(0) = \sigma(0)$.

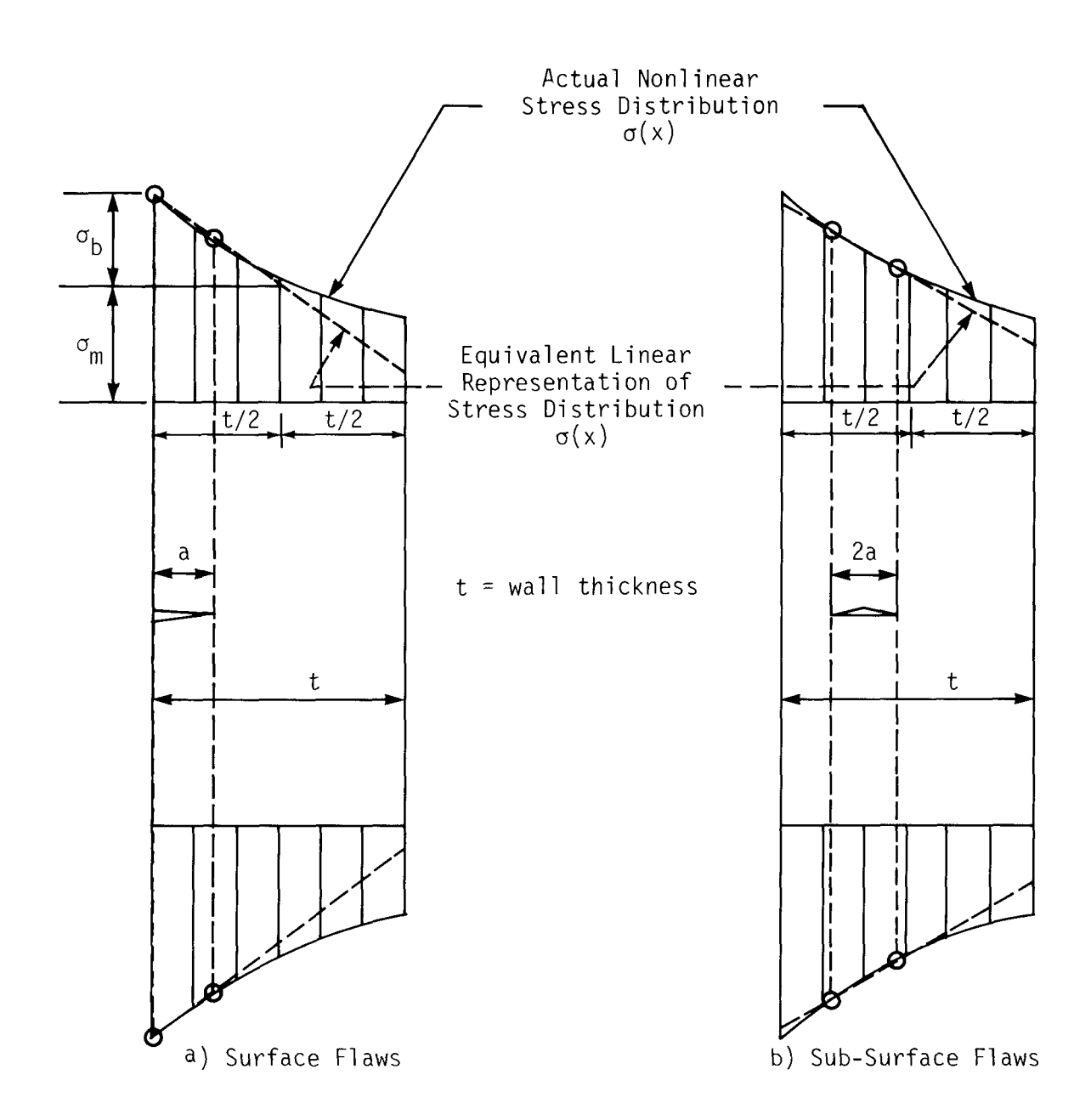


Figure 3.1 - Linearized Representation of Stresses. (Section XI, Fig. A-3200-1)

The membrane and bending portions are simply computed by evaluation Eq. (3.1) at x = (t/2) which yields:

Surface Flaws:

$$\sigma_{\rm m} = \frac{\sigma(a) - \sigma(0)}{a} (t/2) + \sigma(0),$$
 (3.2)

$$\sigma_{\rm b} = \hat{\sigma}(0) - \sigma_{\rm m} = -\frac{\sigma(a) - \sigma(0)}{a} \quad (t/2).$$
 (3.3)

For sub-surface indications, the equivalent linearized stress distribution is determined by substituting the interior flaw positions $x_1 = (x_c - a)$ and $x_2 = (x_c + a)$ into Eq. (3.1). Here x_c is defined as the coordinate of the center of the elliptical flaw shown in Fig. 2.3b. By similar algebraic separation, the membrane and bending components become:

Sub-Surface Flaws:

$$\sigma_{\rm m} = \frac{\sigma(x_{\rm c} + a) - \sigma(x_{\rm c} - a)}{2a} (t/2 - x_{\rm c} + a) + \sigma(x_{\rm c} - a), \quad (3.4)$$

$$\sigma_{\rm b} = \hat{\sigma}(0) - \sigma_{\rm m} = -\frac{\sigma(x_{\rm c} + a) - \sigma(x_{\rm c} - a)}{2a} (t/2).$$
 (3.5)

3.3 Calculation of the Stress Intensity Factor, K_{I}

Article A-3000 of Section XI presents a recommended procedure for determining the stress intensity factor ($K_{\rm I}$). Once the applied stresses at the flaw location are resolved into membrane and bending components with respect to the wall thickness using the equivalent linear representation described in Section 3.2, the Mode I stress intensity factor for the flaw

model is computed from

$$K_{I} = \sqrt{\pi a/Q} \left(M_{m} \sigma_{m} + M_{b} \sigma_{b} \right), \qquad (3.6)$$

where

a = Flaw size defined in Fig. 3.1

Q = Flaw shape parameter

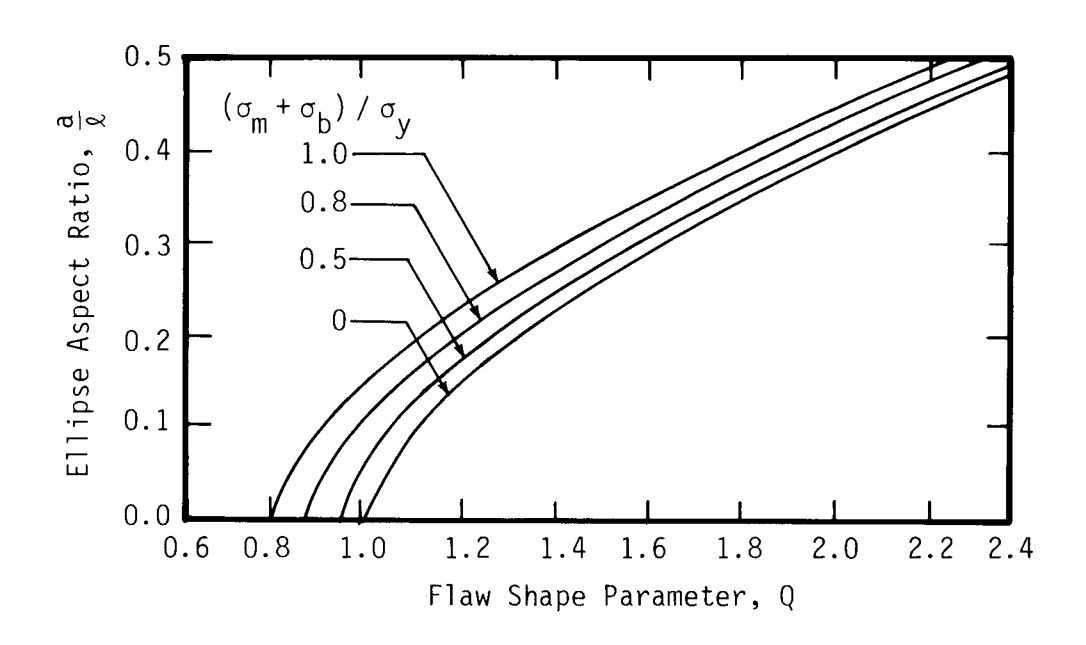
 $M_{\rm m}$ = Free surface correction factor for membrane stresses

 M_b = Free surface correction factor for bending stresses

The parameters Q, $\rm M_m$, and $\rm M_b$ are given in graphical form in Figs. A-3300-1 through A-3300-5 in Article A-3000. These curves are reproduced in this report in Figs. 3.2 through 3.6. Equational forms of Q, $\rm M_m$, and $\rm M_b$ are developed in the Appendix to this report using a combination of analytical and curve fitting techniques. These equations are programmed in the FACET program as function routines to provide a closed form expression for $\rm K_I$ defined by Eq. (3.6). The algorithm for calculating $\rm K_I$ is set up so that if $\rm K_I$ variations exist around the crack front, the maximum value is used in the analysis.

3.4 Selection of Material Properties

The definition of the material properties and the requirements for testing were summarized in Section 2.5. The FACET program has the provision of either accepting user-supplied values of $K_{\rm Ic}$ and/or $K_{\rm Ia}$ and da/dN



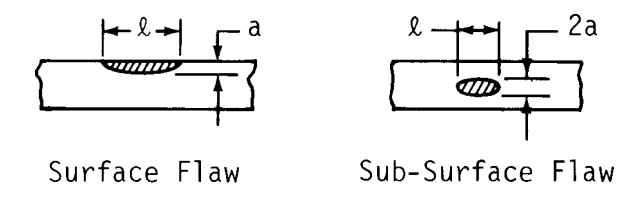


Figure 3.2 - Shape Factor for Flaw Model. (Section XI, Fig. A-2000-1)

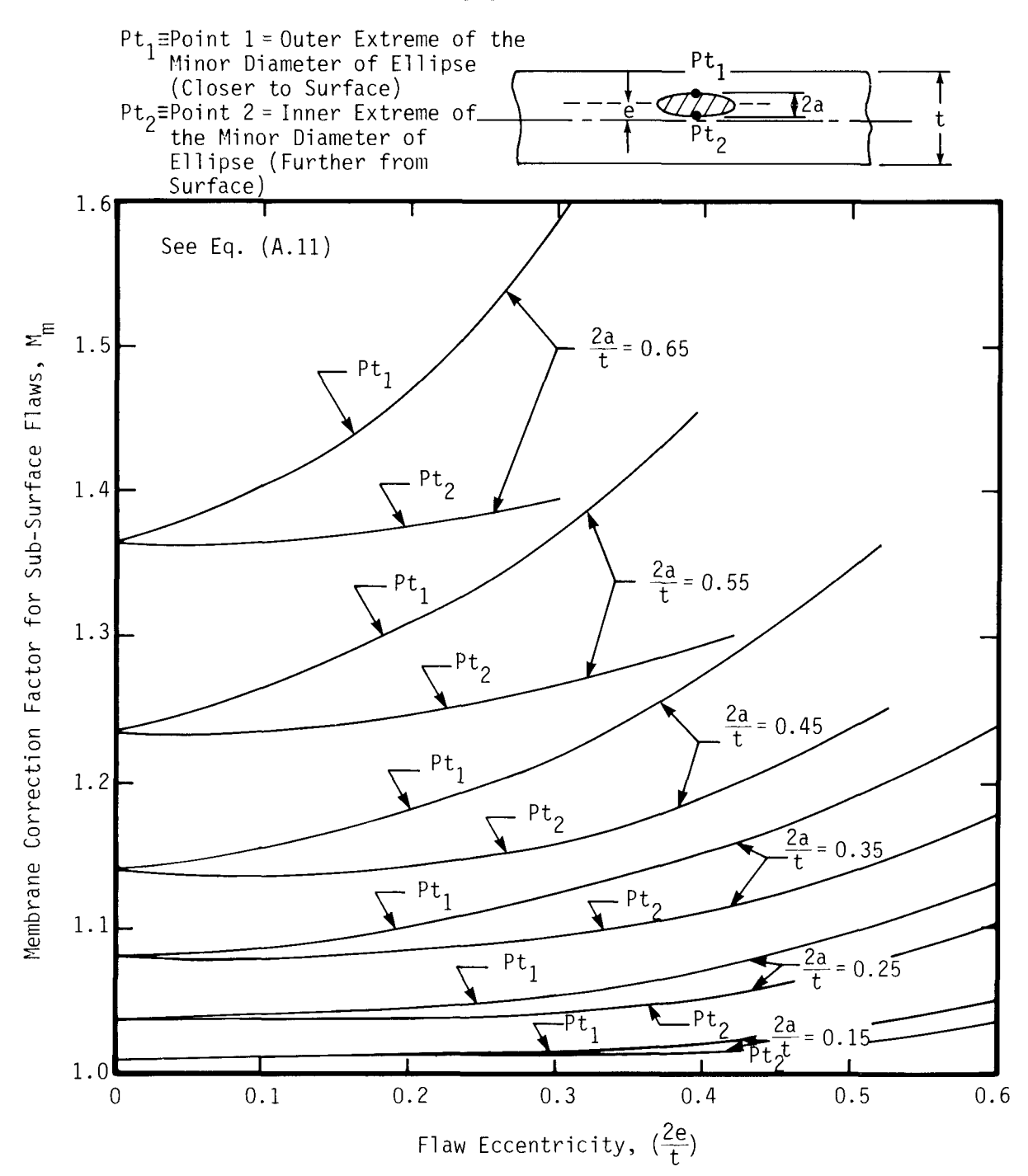


Figure 3.3 - Membrane Correction Factor for Sub-Surface Flaws (From Section XI, Fig. A-3300-2).

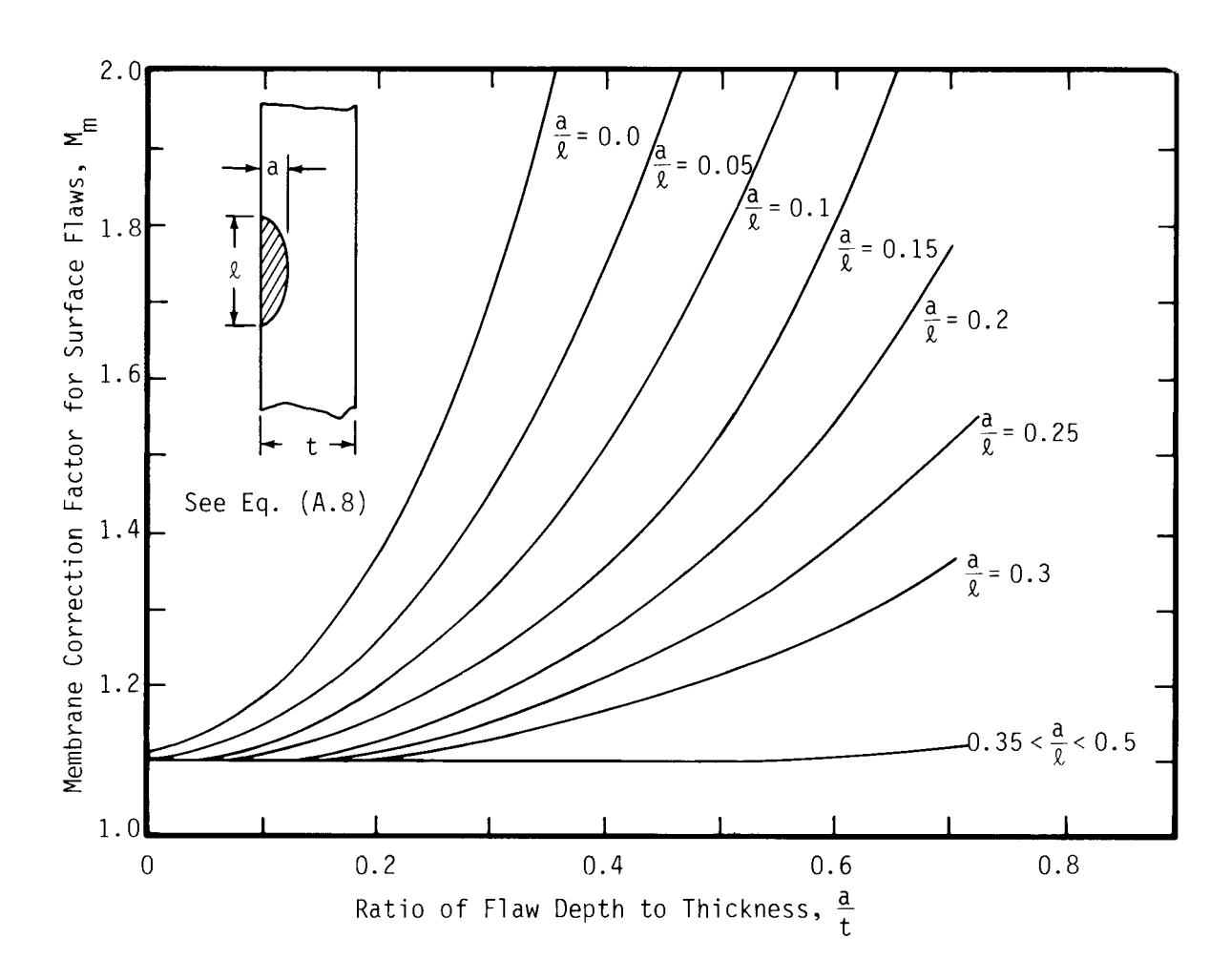


Figure 3.4 - Membrane Correction Factor for Surface Flaws (From Section XI, Fig. A-3300-3).

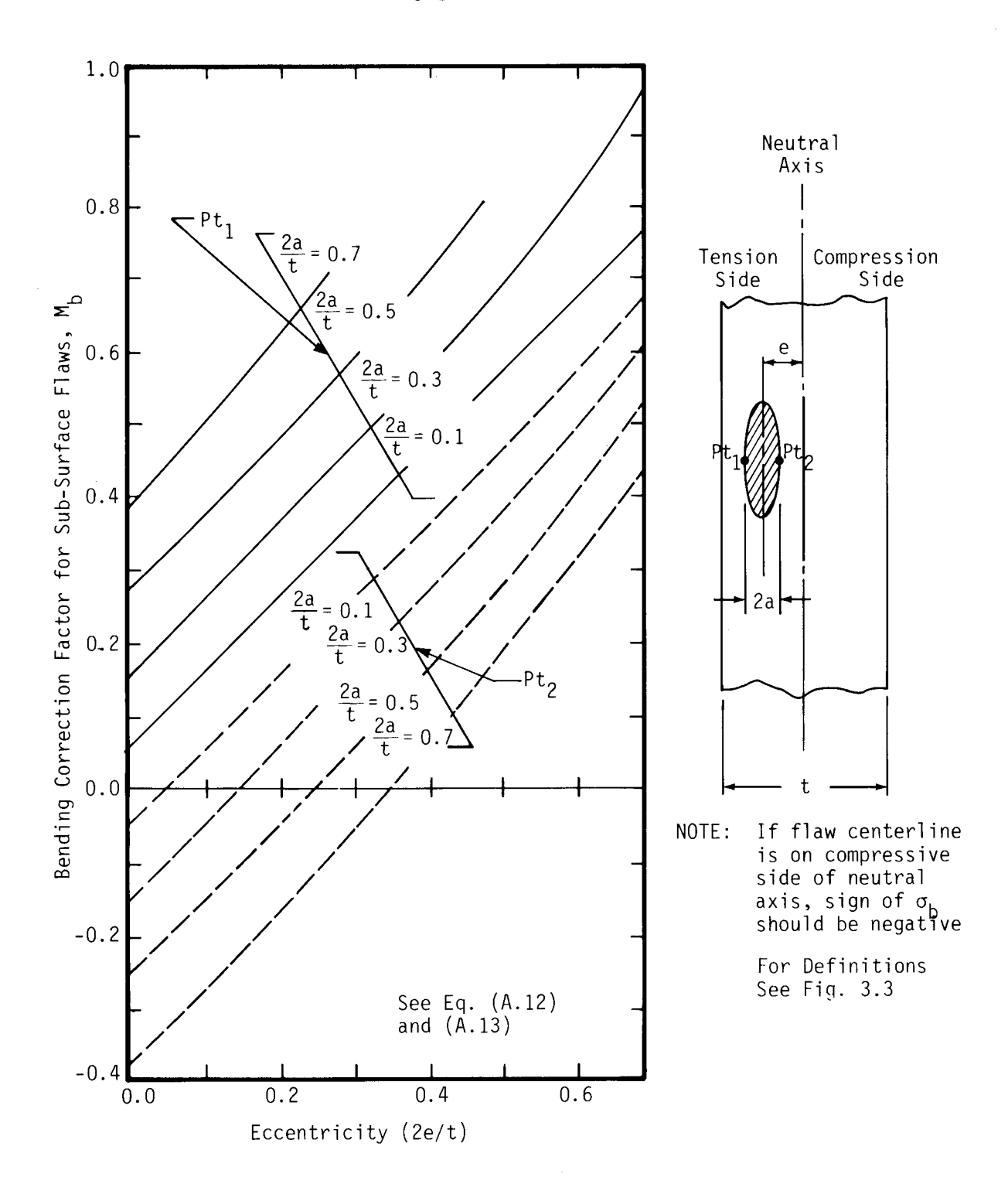


Figure 3.5 - Bending Correction Factor for Surface Flaws (From Section XI, Fig. A-3300-4).

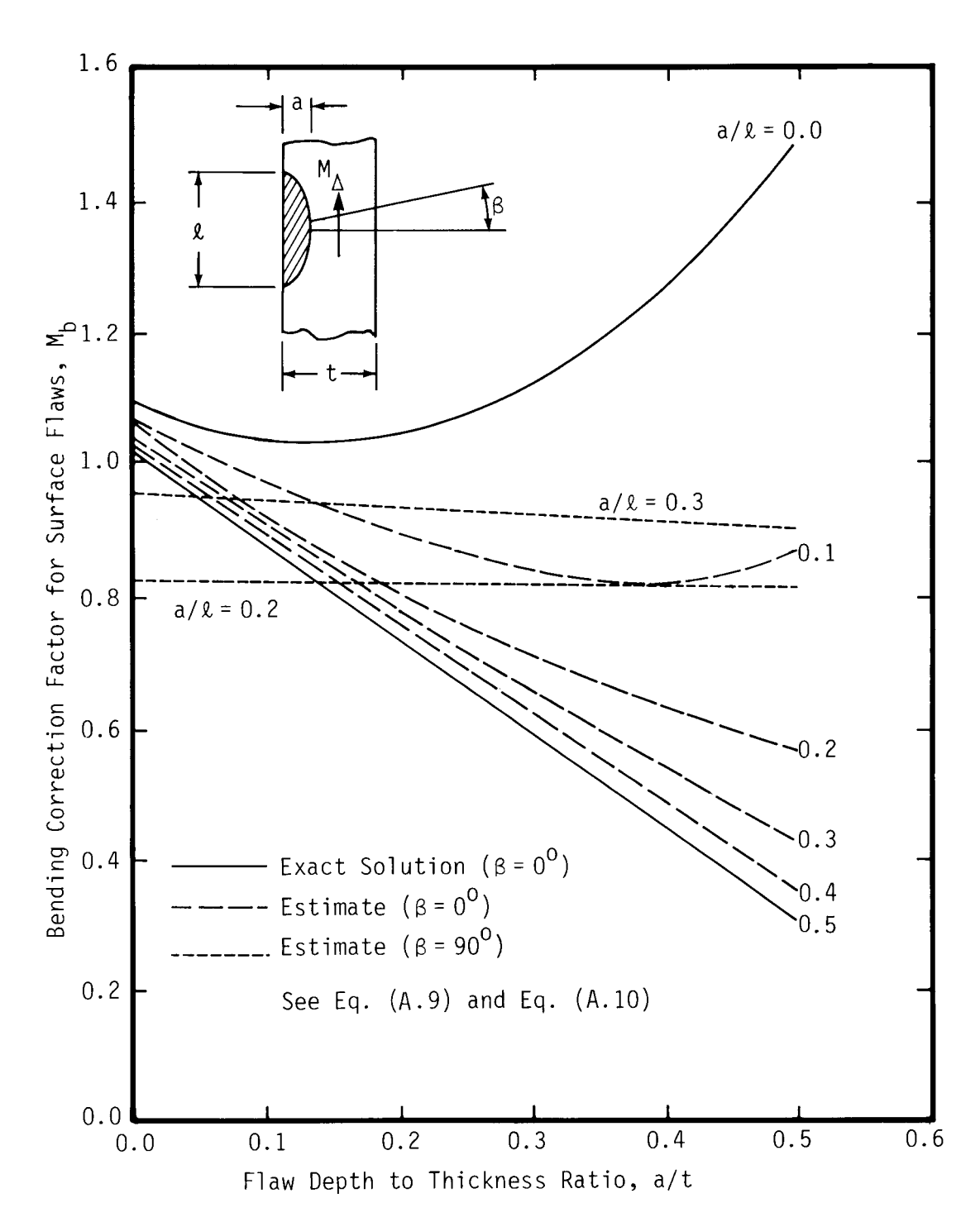


Figure 3.6 - Bending Correction Factor for Surface Flaws (From Section XI, Fig. A-3300-5).

parameters, or using the consevative* values given in Section XI. Similarly, if the effect of irradiation is not available, the shift in material toughness properties as a result of fast neutron fluence and copper content is accommodated by the user specifying as input data ΔRT_{NDT} given in Fig. 2.5 based on the expected end-of-life fluence level at the flaw location.

The da/dN curves provided in Section XI are given in Fig. 2.6. These curves are only conservative for a low R ratio (R = K_{min}/K_{max}) values and caution should be exercised when using the curve for reactor water environment when high R values are expected. If the user elects not to use these curves, FACET provides two input options. The user specifies either C_0 and n in Eq. (2.8) or a table of da/dN versus ΔK points. If the table is input, the program will use a Paris rule, Eq. (2.8), to interpolate between points or for extrapolation outside the tabular range.

3.5 Method of Analysis

3.5.1 <u>Determination of End-of-Life Flaw Size (a_f)</u>

The expected end-of-life flaw size (a_f) is computed by a cumulative fatigue crack growth study for normal operating conditions for the remainder of the expected service life of the component. This procedure is outlined in A-5200 in Section XI. Normal conditions include all transients expected to occur during testing and normal operation. Included in normal operation are upset conditions which are anticipated to occur frequently enough as to warrant their consideration during design. Excluded from the fatigue analysis are all emergency and faulted conditions.

^{*}Conservative means any assumption leading to faster calculated growth rates and/or smaller critical crack sizes than use of reasonable alternative data and analysis.

The FACET program performs the fatigue analysis by rearranging and integrating Eq. (2.8). To increase computational efficiency and prevent costly user input errors, the integration scheme proceeds over a range in crack size from a starting crack depth \mathbf{a}_0 to a final size \mathbf{a}_f , rather than cycle-by-cycle. Hence, the number of applied load cycles N for a given design transient can be defined in terms of \mathbf{a}_f and \mathbf{a}_0 as

$$N = \int_{a_0}^{a_f} \frac{da}{da/dN}, \qquad (3.7)$$

or

$$\delta N = N - \int_{a_0}^{a_f} \frac{da}{da/dN} = 0.$$
 (3.8)

Since the unknown quantity is a_f , Eq. (3.8) is a transcendental expression involving a_f and must be solved using an iterative process. The secant method or method of false positioning (3-1) is used to find the value of a_f which satisfies Eq. (3.8) (i.e., δN = 0) where successive approximations to the i^{th} value of a_f is computed from

$$a_f^{i+1} = a_f^i - \delta N^i (a_f^{i-1} - a_f^i) / (\delta N^{i-1} - \delta N^i).$$
 (3.9)

The iterative process is terminated when either

$$|a_f^i - a_f^{i-1}| \le a_{tol},$$
 (3.10)

or

$$|\delta N^{\dagger}| \leq N_{tol}. \tag{3.11}$$

The tolerance values a_{tol} and N_{tol} are automatically set to 10^{-8} inches and 0.2 cycles, respectively.

All numerical integration is accomplished using one form of Simpson's rule, (3-1)

$$\int_{a}^{b} f(x) dx \simeq \frac{(b-a)}{3k} (f_{0} + 4f_{1} + 2f_{2} + 4f_{3} . . .$$

$$+ 2f_{k-2} + 4f_{k-1} + f_{k}),$$
(3.12)

where k is an even number of uniform step sizes in the x domain. The integration step size (b - a)/k is automatically adjusted based on estimates of the change of ΔK in the interval $\Delta a = b - a$.

3.5.2 <u>Determination of Minimum Critical Flaw Size (a_C)</u>

The procedure to compute the minimum critical flaw size for normal operation (a_c) is specified by Article A-5200. This procedure is outlined below:

(1) Determine the maximum end-of-life irradiation level at the flaw location

- (2) Using irradiated fracture toughness data, determine the crackarrest fracture toughness (K_{Ia}) as a function of temperature
- (3) Calculate stress intensity factors, $K_{
 m I}$, for various geometrically similar crack depths of the assumed flaw
- (4) Compare the calculated stress intensity factors to the material fracture toughness (K_{Ia}) for the appropriate temperature to determine the critical flaw size (a_{C}) for the transient
- (5) Proceed to the next transient

The procedure to compute a_{C} is illustrated schematically in Fig. 3.7. The variation of K_{Ia} with temperature is used to compute a value of K_{Ia} corresponding to the metal wall temperature for each transient of normal operation. The temperature value used in this computation is the temperature which exists at the crack tip, as determined from the through-wall temperature distribution for each transient condition. The calculated values for the stress intensity factor as a function of crack depth, $K_{I}(a)$, are utilized in the determination of a_{C} from

$$K_{I}(a_{c}) = K_{Ia}(T(a_{c}), RT_{NDT}, \Delta RT_{NDT}),$$
 (3.13)

which represents the intersection of the toughness distribution and the applied ${\rm K_I}$ field. The smallest value of ${\rm a_c}$ determined by the above procedure after all transients have been considered is the minimum critical flaw size for normal operation. This minimum value of ${\rm a_c}$ is checked against the flaw acceptability criteria of Paragraph IWB-3600 (see Section 2.3).

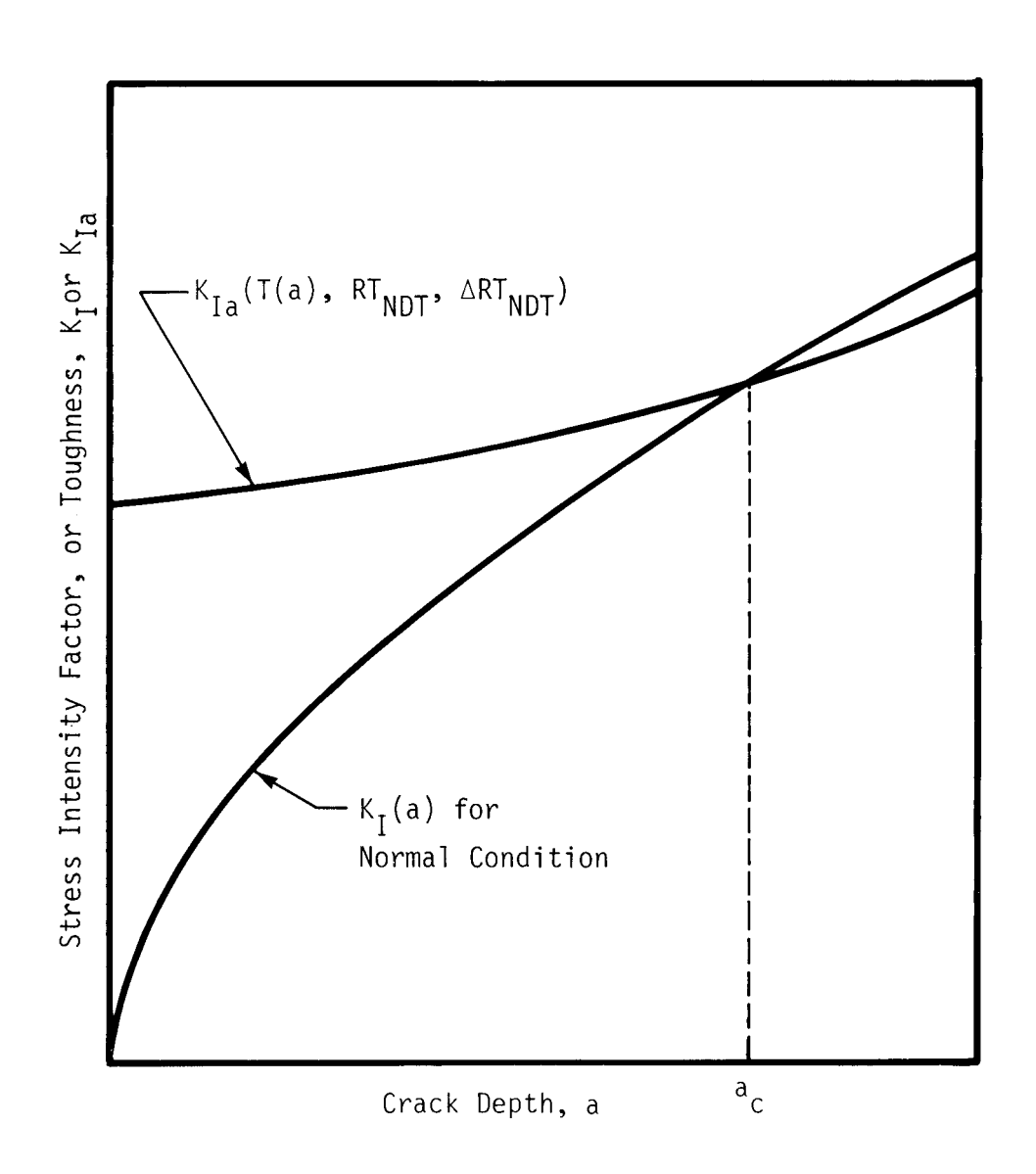


Figure 3.7 - Determination of a Critical Flaw Size, $a_{\rm C}$, for Normal Conditions.

3.5.3 <u>Determination of Minimum Critical Flaw Size for Initiation (a;)</u>

The procedure to determine the minimum critical flaw size for initiation of a non-arresting running crack caused by an emergency or faulted transient conditions is specified by Article A-5300. As specified in A-5300, each postulated incident should be considered for critical flaw size as follows:

- (1) Determine the maximum end-of-life irradiation profile through the thickness of the component at the observed flaw location
- (2) Determine temperature and stress profiles through the thickness of the component at the observed flaw location as a function of time following the postulated incident
- (3) Using the irradiated fracture toughness data, determine the crack arrest (K_{Ia}) and crack initiation (K_{Ic}) fracture toughness profiles through the thickness of the component as a function of time following the postulated incident
- (4) Calculate stress intensity factors (using the methods outlined in A-3000 or some other documented procedure) for various penetration depths of an assumed flaw that is geometrically similar to the ellipse or semi-ellipse that bounds the observed flaw
- (5) The crack penetration at which the calculated stress intensity factor exceeds the $K_{\rm Ic}$ profile corresponds to the critical crack size for initiation (a_i) and the penetration at which the stress intensity factor goes below the $K_{\rm Ia}$ curve corresponds to the critical crack size for arrest (a_a) . This comparison is

illustrated in Fig. A-5300-1 and reproduced in Fig. 3.8 for both an arrest and a nonarrest situation.

As shown in Fig. 3.8, the crack penetration at which the applied ${\rm K_I}$ level exceeds ${\rm K_{Ic}}$ corresponds to the critical crack size for initiation $({\rm a_i})$, and the penetration at which ${\rm K_I}$ falls below the ${\rm K_{Ia}}$ curve corresponds to the critical crack size for arrest $({\rm a_a})$. Hence, ${\rm a_i}$ and ${\rm a_a}$ are computed from

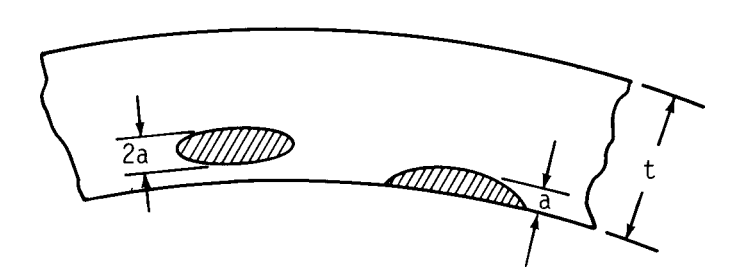
$$K_{I}(a_{i}) = K_{IC}(T(a_{i}), RT_{NDT}, \Delta RT_{NDT}), \qquad (3.14)$$

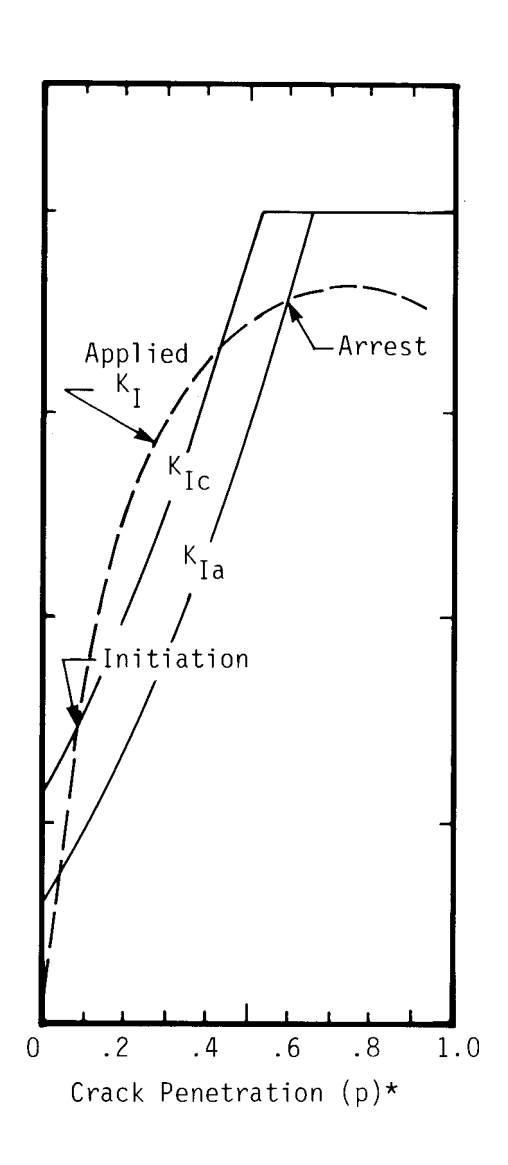
$$K_{I}(a_{a}) = K_{Ia}(T(a_{a}), RT_{NDT}, \Delta RT_{NDT}),$$
 (3.15)

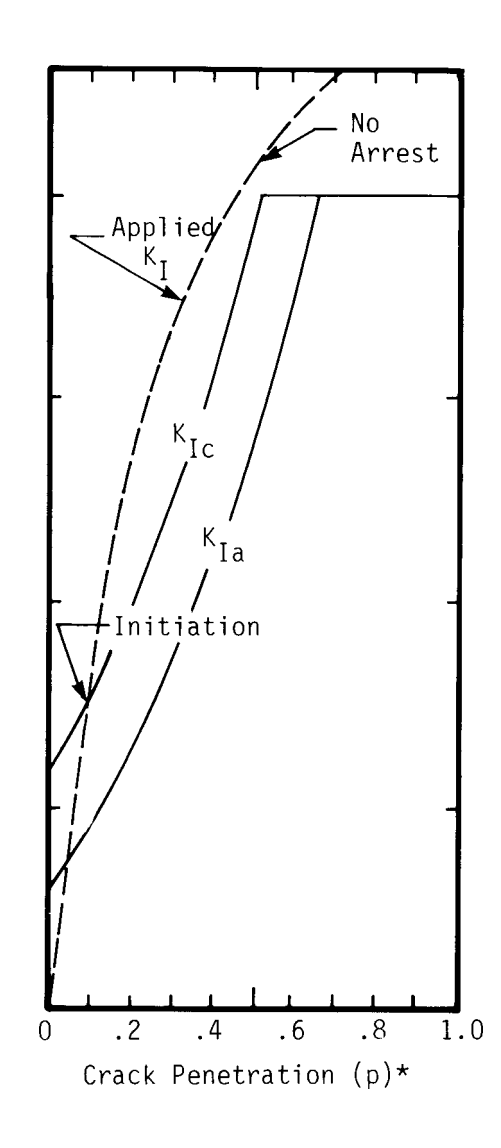
which represent the intersection points of the applied $\rm K_I$ curve with $\rm K_{Ic}$ and $\rm K_{Ia}$ toughness distributions. The smallest value of $\rm a_i$ determined from Eq. (3.14) and for which the crack-arrest penetration (p = $\rm a_a/t$) is greater than 0.75, after all postulated accidents have been considered, represents the minimum critical initiation flaw size for emergency and faulted conditions. This minimum value of $\rm a_i$ is checked against the flaw acceptability criteria of Paragraph IWB-3600 (see Section 2.3).

*For Sub-Surface Flaws: p = 2a/t For Surface Flaws:

For Surface Flaws: p = a/t







- a) Example of Arrest Configuration
- b) Example of Non-Arrest Configuration

Figure 3.8 - Determination of Critical Flaw Sizes for Postulated Conditions (Section XI, Fig. A5300-1).

REFERENCES

3-1 Kreyszig, E. <u>Advanced Engineering Mathematics</u>, 3rd Ed., New York, John Wiley & Sons Publishers (1972).

4.0 PROGRAM CAPABILITIES AND RESTRICTIONS

4.1 Data Input Description

A summary of the data card input for the FACET program is given in Table 4.1. Each of the eight card series labeled A through H defines a specific segment of the input data. The Title Card (Card A) gives the user an 80-character heading for the program which will be printed at the top of each output page. The Control Card (Card B) defines the parameters which are associated with the type of problem, the problem size, and input options. The user or analyst has several options as to the type of analysis to be run. The options are listed below:

- (1) Data check only
- (2) Evaluation of K_{I} as a function of crack depth for the userspecified transient stress distributions only
- (3) Cumulative fatigue analysis to determine a_f only
- (4) Cumulative fatigue analysis to determine a_f and static toughness calculation to determine a_c and a_i
- (5) Static toughness calculation to determine a_c and a_i only

The details regarding the initial flaw dimensions and positions are given in the Geometry Card (Card C). The material properties are defined using the Material Data Card (Card Series D). The conservative bounds on fracture toughness and crack growth rate data are built into the program and will be used if actual properties are not specified. For this case, only

TABLE 4.1 CARD INPUT DESCRIPTION FOR FACET

CARD SERIES ID	SUB SERIES	CARD DESCRIPTION
Α		Title Card
В		Control Card
С		Geometry Card
D		Material Data
	D1 D2 D3	Material Data Card Crack Growth Rate Data Fracture Toughness Data
E		Stress Distribution Data
	E1 E2	Stress Data Title Card Tabular Stress Data
F		Temperature Distribution Data
	F1 F2	Temperature Data Title Card Tabular Temperature Data
G		Transient Data
	G1 G2	Transient Condition and Title Transient Steps, Temperature, and Stress Definition
Н		Job Termination Card

Card D1 is needed. If the user has available actual material data which meets the requirements of A-4000, Card Series D2 is used to input fracture toughness data versus temperature in tabular form.

The stress distribution, temperature distribution, and transient data follow next in Card Series E, F, and G. The stress and temperature data are specified in sets; each set is a table of points of stress or temperature versus through-wall position. Each data set has its own Title Heading Card. The transient data cards define the type of transient condition (normal/upset, test, emergency, or faulted), the number of constant amplitude load steps, and the number of expected transient occurrences in the remaining service life. These inputs are defined on Card G1. Next, the indices which define the temperature and stress distributions, and the number of cycles for each load step are specified on Card G2.

The last card (Card H) is the Job Termination Card which defines the completion of the input data to the problem. Additional problems can be stacked behind the first run for multiple job execution.

4.2 <u>Problem Execution and Output</u>

FACET reads, executes, and prints each problem before proceeding onto the next problem. All input data is first checked and printed before the problem is actually solved. During the analytical portion, important intermediate results are printed immediately after they have been calculated. Any mistakes discovered during data input or problem solution will result in the printing of a message. FACET provides two types of output messages, warning, and error. The warning message system alerts the user of possible mistakes without terminating problem execution. The general areas where warning

messages apply are

- (1) Input and certain problem parameters which violate the intended scope of the Section XI evaluation procedure
- (2) Potential inaccuracies of calculated quantities

Certain mistakes discovered before or during the analytical portion will result in an error message and problem termination. Error messages and termination of execution occur for

- (1) All user input errors
- (2) Entrance of certain parameters into a domain where the Code procedure is inapplicable

After the error message is printed, the program will skip to the next problem in the data set.

4.3 Problem Size Limits

The present limits on the primary input parameters which affect the problem size are summarized in Table 4.2. The limits shown in Table 4.2 were chosen during the development of the program, hence, they are somewhat arbitrary. Since FACET has a small core memory requirement, these limits can be increased easily, if warranted.

TABLE 4.2 PRESENT LIMITS ON PROBLEM SIZE IN FACET

VARIABLE NAME	DESCRIPTION	LIMIT
NSIG	Number of Stress Distributions	40
NSPTS	Number of Point Values Per Stress Distri- bution	20
NTEMP	Number of Temperature Distributions	40
NTPTS	Number of Point Values Per Temperature Distribution	20
NTRAN	Number of Transients	40
NSTEPS	Number of Loading Steps Per Transient	10
NKPTS	Number of K _I Values Computed in K Analysis	30
NDADN	Number of da/dN Versus ΔK Points	20
NKIA	Number of K _{Ia} Versus Temperature Points	20
NKIC	Number of $K_{f Ic}$ Versus Temperature Points	20

5.0 SIMPLE EXAMPLE PROBLEM

A simple fatigue analysis problem of a part-through elliptical surface crack in a large pressure vessel subjected to only pressure cycles is presented to demonstrate the capabilities of FACET. The purpose of this example problem is to compute the final flaw size a_f . The flaw is assumed to be located in a stress region where both membrane ($\Delta\sigma_m$ = 10 ksi) and bending ($\Delta\sigma_b$ = 8 ksi) exist. The detected flaw depth is 0.10" in an 8-inch vessel wall, and the crack aspect ratio is a/2c = 1/6. The material yield strength is 50 ksi, and the Code da/dN behavior for reactor water environment is assumed. The problem is to determine the final flaw size after 50 x 10^3 cycles.

As part of the analysis, the variation in ΔK as a function of crack depth is computed. These results are plotted in Fig. 5.1. The increase in crack depth as a function of applied cycles is shown in Fig. 5.2. For illustrative purposes, the fatigue analysis was extended beyond 50 x 10^3 cycles. The final flaw depth at 50 x 10^3 cycles is computed to be $a_f = 0.674$ inches. Additional sample problems which demonstrate other program features are provided in the User's Manual (1-3).

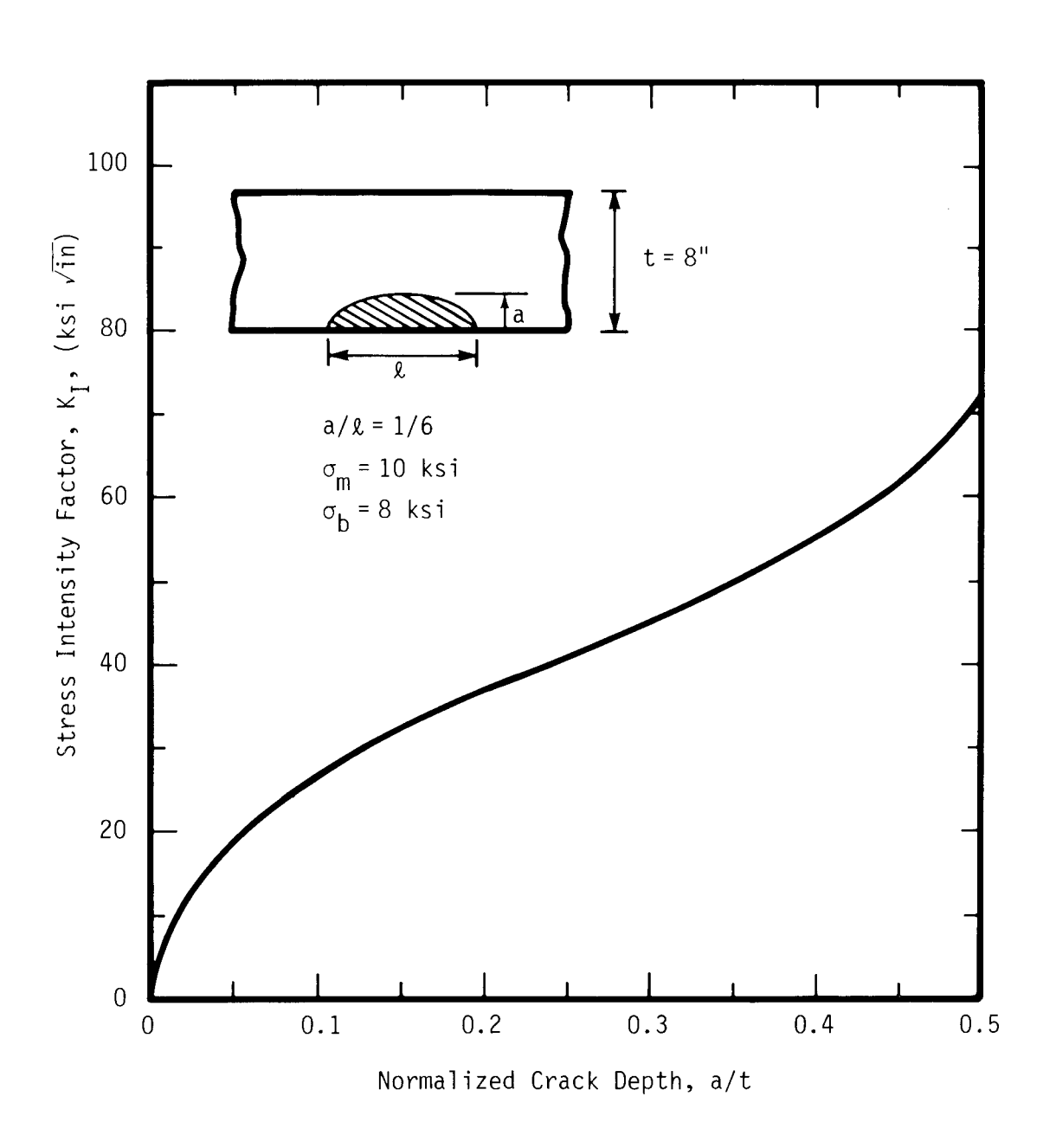


Figure 5.1 - Calculated Stress Intensity Factor versus Crack Depth.

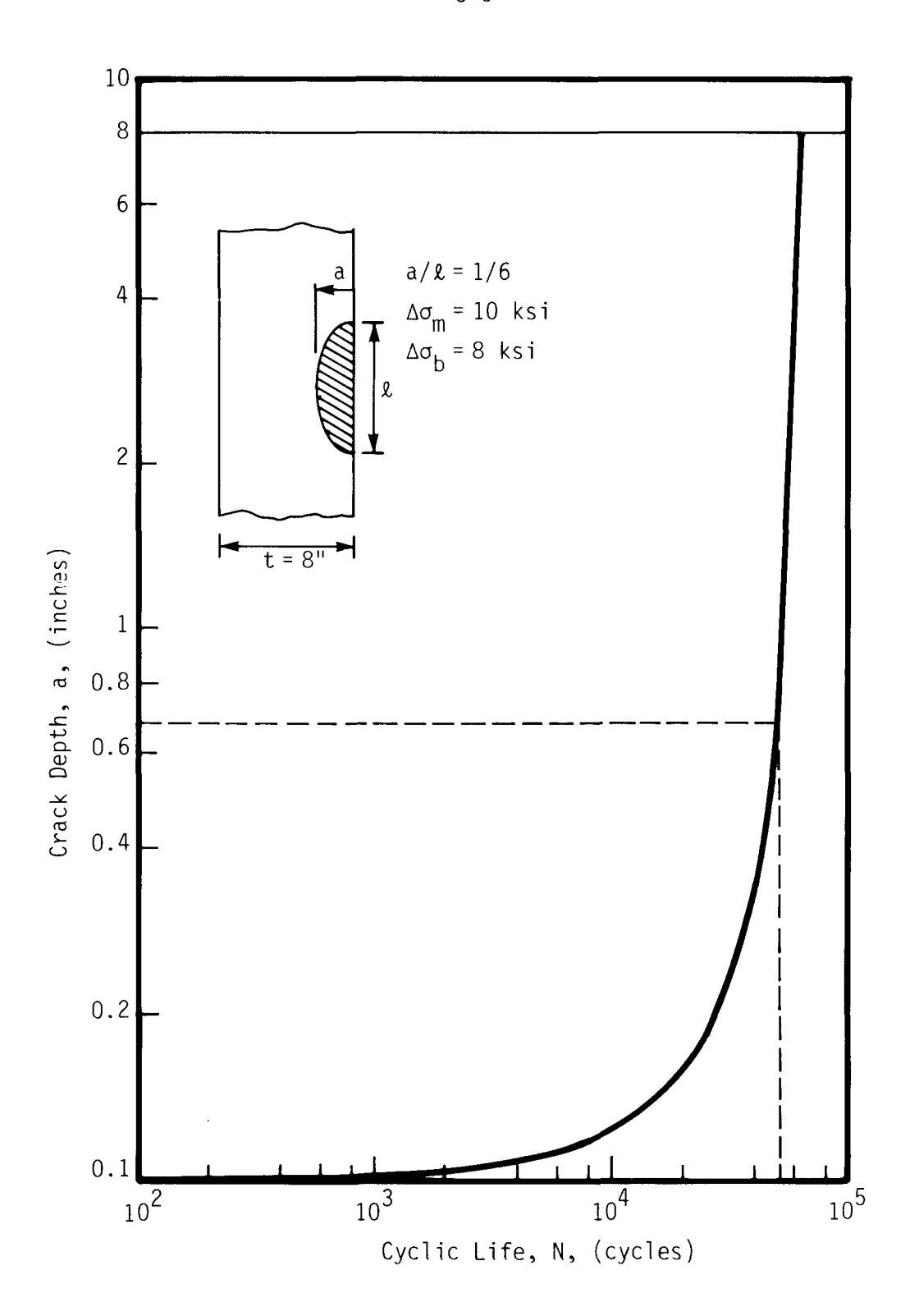


Figure 5.2 - Calculated Crack Depth versus Applied Cycles.

6.0 SUMMARY AND CONCLUSIONS

- (1) A computer program called FACET has been developed which performs all the calculations required for Section XI, Appendix A of the ASME Boiler and Pressure Vessel Code.
- (2) Closed form relations for computing the flaw shape parameter Q, and the free surface correction factors in tension and bending, $M_{\rm m}$ and $M_{\rm b}$ have been developed and are programmed in FACET.
- (3) The program and related documentation are generally available.

7.0 REFERENCES

- A-1 "PVRC Recommendations on Toughness Requirements for Ferritic Materials," Welding Research Council Bulletin, No. 175 (August 1972).
- A-2 Green, A. E. and I. N. Sneddon. "The Stress Distribution in the Neighborhood of a Flat Elliptical Crack in an Elastic Solid," <u>Proceedings</u>, Cambridge, Phi., Soc., Vol 46 (1950).
- A-3 Irwin, G. R. "Characterization of Part-Through Cracks in Tension," In The Surface Crack: Physical Problems and Computational Solutions, ASME (1972).
- A-4 Irwin, G. R. "Crack Extension for a Part-Through Crack in a Plate," Journal of Applied Mechanics, 29, Trans. ASME, 84 (1962), Pp. 651-654.
- A-5 Dwight, H. B. <u>Table of Integrals and Other Mathematical Data</u>, Macmillan Company (1961).
- A-6 Wilhelm, D. P. "Fracture Mechanics Guideline for Aircraft Structural Applications," AFDL-TR-69-11, Northrup Corporation (February 1970).
- A-7 Smith, F. W. "Stress Intensity Factors for a Semi-Elliptical Surface Flaw," Struct. Develop. Res. Memo No. 17, Boeing Company (August 1966).
- A-8 Tada, H., P. Paris, and G. Irwin. "The Stress Analysis of Cracks Handbook," Del Research Corporation (1973).
- A-9 Kobayashi, A. S., M. Ziv, and L. R. Hall. "Approximate Stress Intensity Factor for an Embedded Elliptical Crack Near Two Parallel-Free Surfaces," <u>International Journal of Fracture Mechanics</u>, 1 (1965), Pp. 81.
- A-10 Shah, R. C. and A. S. Kobayashi. "Stress Intensity Factor for an Elliptical Crack Approaching the Surface of a Plate in Bending," ASTM STP 513 (1972), Pp. 3.

APPENDIX A

EQUATIONS TO COMPUTE K_{T} USING RECOMMENDED CODE PROCEDURE

A.1 INTRODUCTION

As introduced in Section 3.3, the calculation of the Mode I stress intensity factor, $K_{\rm I}$, is accomplished using the procedures of Article A-3000. General background information to Article A-3000 is provided in (A-1). The equational form for $K_{\rm I}$ is given by Eq. (3.1) and is rewritten below as

$$K_{I} = \sqrt{\pi a/Q} \left(M_{m} \sigma_{m} + M_{b} \sigma_{b} \right), \qquad (A.1)$$

where

a = Flaw size

Q = Flaw shape parameter

 $M_{\rm m}$ = Free surface correction factor for membrane stresses

 M_h = Free surface correction factor for bending stresses

The parameters Q, $\rm M_m$, and $\rm M_b$ are given in graphical form in Figs. A-3300-1 through A-3300-5 in Article A-3000, which are reproduced in Figs. 3.2 through 3.6 in Section 3.0. To express completely $\rm K_I$ in a functional form, equations for the determination of Q, $\rm M_m$, and $\rm M_b$ in terms of simple quantities are needed. Contained in this Appendix are equational forms for Q, $\rm M_m$, and $\rm M_b$ and a description of the technique used to formulate them. These equations are programmed in the FACET program as function routines and allow a direct calculation of $\rm K_T$ in Eq. (A.1).

A.2 THE FLAW SHAPE PARAMETER, Q

A.2.1 General Description

The effect of the ratio of crack depth to length for elliptical-shaped flaws is accounted for by the flaw shape parameter, Q. The elastic analysis of flat elliptical flaws originated with Green and Sneddon ($\underline{A-2}$). For the case of part-through cracks in plates, Irwin ($\underline{A-3}$) suggests that the flaw shape parameter, taking into account a plasticity correction factor to the crack size, can be characterized by

$$Q = E_k^2 - 0.212 (\sigma/\sigma_v)^2,$$
 (A.2a)

$$k^2 = 1 - 4 (a/\ell)^2$$
, (A.2b)

where σ/σ_y is the ratio of the gross tensile stress to yield strength. The tensile stress σ is defined by the Code as the sum of the resolved membrane and bending components as

$$\sigma = \sigma_{\rm m} + \sigma_{\rm h} . \tag{A.2c}$$

The plastic correction term (i.e., the second term in Eq. (A.2a)) is equivalent to the assumption that the crack length is longer than the measured or actual crack depth by the length of the plastic zone directly ahead of the crack. By using this plastic correction term in the computations of ΔK for fatigue, crack growth calculations will be conservative since no account is made for the crack to unload and, subsequently, to reload elastically under cyclic conditions (i.e., non-monotonic conditions within a loading range of approximately twice the yield strength). Hence, for fatigue calculations in which elastic shakedown occurs, a case could be made for defining $\sigma_{\bf y}$ as the

sum of absolute compressive and tensile yield strengths. Section XI presents Eq. (A.2) in graphical form (Fig. A-3300-1) for a range of a/ ℓ and $(\sigma_{\rm m} + \sigma_{\rm b})/\sigma_{\rm y}$ values as reproduced in Fig. 3.2.

A.2.2 Numerical Determination of Q

To compute Q from Eq. (A.2), the elliptic integral, E_k , can be evaluated using an infinite series given by Dwight (A-4). After some manipulation, this series can be expressed as

$$E_{k} = 1 + \frac{m^{2}}{4} + \sum_{n=2}^{\infty} \frac{(2n-2)! m^{2n}}{(2n)2^{2(n-1)} [(n-1)!]^{2}}, \quad (A.3a)$$

where

$$m = \frac{1 - (1 - k^2)^{\frac{1}{2}}}{1 + (1 - k^2)^{\frac{1}{2}}}.$$
 (A.3b)

By retaining the first six terms in Eq. (A.3a), the maximum error in E_k is 0.1%, which occurs when m is equal to unity. Substitution of Eq. (A.4) and Eq. (A.3b) into Eqs. (A.2a) and (A.2b), respectively, yields the desired numerical expression for Q and m:

$$Q \simeq \frac{\pi^2}{4(1+m)^2} \left[1 + \frac{m^2}{4} + \frac{m^4}{64} + \frac{m^6}{256} + \left(\frac{5}{128}\right)^2 m^8 + \left(\frac{7}{256}\right)^2 m^{10} \right]^2$$

-
$$0.212(\sigma/\sigma_y)^2$$
, (A.4a)

$$m = \frac{1 - 2(a/\ell)}{1 + 2(a/\ell)} . \tag{A.4b}$$

A.3 FREE SURFACE CORRECTION FACTORS

A.3.1 General Description

Theoretical solutions exist for the variation in K around an embedded flaw; however, when the crack becomes deep with respect to the thickness of the plate, the free surface tends to elevate the actual stress intensity factor to levels greater than the infinite plate solutions (K_{Ie}). Investigators have approached the finite body problem by developing multiplying factors which will "correct" the infinite problem to account for finite width effects. For example, for the case of a surface flaw in a finite plate of thickness, t, under tension, Irwin ($\underline{A-5}$) estimated the effect of the two free surfaces to be $M_m=1.1$, or

$$K_{I} = 1.1 K_{Ie}.$$
 (A.5)

This expression correlates reasonably well with experiments and more recent analyses of nearly semicircular flaws only for ratios of a/t < 0.5. Many investigators have resorted to using numerical analysis for computing K for cracks in finite bodies. Wilhelm ($\underline{A-6}$) presents the results of several recent surface crack analyses in the form of "correction factors" for various values of a/t. Section XI gives these correction factors in graphical form in Figs. A-3300-2 through A-3300-5, which are reproduced in Figs. 3.3 through 3.6 of this report.

A.3.2 Curve Fitting of $M_{\rm m}$ and $M_{\rm b}$ for Surface Flaws

The original source of $\rm M_m$ and $\rm M_b$ for surface flaws was given in Figs. A-3000-3 and A-3000-5 is based on the analysis of Smith (A-7) and reproduced by Wilhelm (A-6). The variation in $\rm M_b$ around the crack front

 $(B=0^{\circ}, 90^{\circ})$ is partially included in the curves. To obtain functional forms for M_{m} and M_{b} , the data given in Figs. 3.3 through 3.6 were curve fitted using a multi-variable least squares method. For surface flaws, the curve-fitting process was simplified by using two intermediate functions for K or infinitely long flaws $(a/\ell = 0)$ tabulated by Tada, et. al. $(\underline{A-8})$. For the uniform pressure and bending applied stress fields, these functions, in terms of a/t and $\phi = (\pi a/2t)$, are

$$F_{\rm m}(a/t) = 0.265 (1 - a/t)^4 + \frac{0.857 + 0.265(a/t)}{(1 - a/t)^{3/2}}$$
, (A.6)

$$F_b(a/t) = \left[(1/\phi) \ \text{Tan } \phi \right]^{\frac{1}{2}} \frac{0.923 + 0.199 (1 - \sin \phi)^4}{\cos \phi} \cdot (A.7)$$

The accuracy of Eqs. (A.6) and (A.7) is reported by (<u>A.6</u>) to be better than 1% for F_m and better than 0.5% for F_b for any a/t. Equations (A.6) and (A.7) were than used as multiplying factors in the general functional relations evaluated by the curve-fit program. The dependence of the correction factors M_m and M_b on a/ ℓ was evaluated by fitting data points from the Code graphs: approximately 106 points for M_m (Fig. 3.4) and 118 points for M_b (Fig. 3.6). Curves for determining M_b on the major and minor crack fronts of the ellipse (β = 90° and 0°, repectively) were fit. After several trials with the curve-fit process, the following expressions for the correction factors were obtained.

Surface Flaw in Tension ($\beta = 0$ or Point Pt₁)

$$M_{m} = A_{1} + F_{m} \left\{ \left[A_{2} + A_{3}(a/\ell) + A_{4}(a/t)(a/\ell) \right] + (a/\ell)^{1/3} \left[A_{5}(a/t) + A_{6}(a/t)^{2} + A_{7}(a/t)^{3} + A_{8}(a/t)^{4} \right] + A_{9}(a/t)(a/\ell)^{\frac{1}{2}} \right\}$$

$$(A.8a)$$

where

$$A_1 = -0.05314636$$
 $A_5 = 2.998569$
 $A_2 = 1.071457$ $A_6 = -5.357526$
 $A_3 = -0.2136716$ $A_7 = 6.75775$
 $A_4 = 4.369957$ $A_8 = -2.545777$
 $A_9 = -6.520983$

for $0 \le a/\ell \le 0.25$, and for $0.25 < a/\ell \le 0.5$

$$M_{m} = A_{1}^{'} + F_{m}A_{2}^{'} + A_{3}^{'}(a/\ell) + A_{4}^{'}(a/t)(a/\ell)$$

$$+ (a/\ell)^{1/3} \left[A_{5}^{'}(a/t) + A_{6}^{'}(a/t)^{2} + A_{7}^{'}(a/t)^{3} + A_{8}^{'}(a/t)^{4} \right]$$

$$+ A_{9}^{'}(a/t)(a/\ell)^{\frac{1}{2}}$$
(A.8b)

where

$$A_{1}^{'} = 0.8399496$$
 $A_{2}^{'} = 0.01988405$
 $A_{6}^{'} = -1.645873$

$$A_3^{\dagger} = 0.7782449$$
 $A_7^{\dagger} = 5.047168$
 $A_8^{\dagger} = -3.640808$
 $A_0^{\dagger} = 28.01397$

and the limits on a/t are shown in Fig. 3.4.

Surface Flaw in Bending ($\beta = 0$ or Point Pt₁)

$$M_{b} = B_{1} + F_{b} \left\{ \left[B_{2} + B_{3}(a/\ell) + B_{4}(a/t)(a/\ell) \right] + (a/\ell)^{1/3} \left[B_{5} + B_{6}(a/t) + B_{7}(a/t)^{2} + B_{8}(a/t)^{3} + B_{9}(a/t)^{4} \right] + B_{10}(a/t)(a/\ell)^{\frac{1}{2}} \right\}$$

$$(A.9)$$

where

$$B_1 = 0.1976165$$
 $B_6 = 3.70567$ $B_2 = 0.8328891$ $B_7 = -2.385941$ $B_3 = 0.1524948$ $B_8 = 2.171827$ $B_4 = 3.144613$ $B_9 = 0.6973028$ $B_5 = -0.1941165$ $B_{10} = -7.650728$

for $0 \le a/\ell \le 0.5$ and $0 \le a/t \le 0.5$ as shown in Fig. 3.6.

Surface Flaw in Bending ($\beta = 90^{\circ}$ or Point Pt₂)

$$M_{h} = C_{1} + C_{2}(a/\ell) + C_{3}(a/t)$$
 (A.10)

where

 $C_1 = 0.6143659$

 $C_2 = 1.112532$

 $C_3 = -0.07249826$

for $0.2 < a/\ell < 0.3$ and $0 \le a/t \le 0.5$.

A.3.3 Curve Fitting of $M_{\rm m}$ and $M_{\rm b}$ for Sub-Surface Flaws

The curves for ${\rm M_m}$ as a function of relative flaw depth (2a/t) and eccentricity (2e/t) as given in Fig. A-3300-2 were taken from Wilhelm (<u>A-6</u>), who reported the results of Kobayashi, Ziv, and Hall (<u>A-9</u>). The original source for ${\rm M_b}$ as given in Fig. A-3300-4 is Shah and Kobayashi (A-10). Although not stated in the Code or in (<u>A-6</u>), the curves for ${\rm M_m}$ and ${\rm M_b}$ are for a flaw shape of a/ ℓ = 0 (i.e., "tunnel crack geometry"). Kobayashi, et. al., (<u>A-9</u>) gives another multiplying factor on ${\rm M_m}$ to obtain ${\rm M_m}$ for other values of a/ ℓ , however, this factor is always less than unity so that the curves in Section XI are conservative when used for other flaw shapes within the limits of the approximate solution. For bending, (<u>A-10</u>) indicates a small increase (10%) in ${\rm M_b}$ as a/ ℓ increases from zero to one-half.

<u>Sub-Surface Flaw in Tension (Points Pt₁ and Pt₂)</u>

For the embedded flaw in tension, the equations formulated in $(\underline{A-9})$ were programmed directly in FACET. With a slight modification this equation is presented below.

$$M_{m} = \left[D_{1} + D_{2}(2a/t)^{2} + D_{3}(2a/t)^{4} + D_{4}(2a/t)^{6} + D_{5}(2a/t)^{8} + D_{6}(2a/t)^{20} / (1 - 2e/t - 2a/t)^{\frac{1}{2}} \right]$$
(A.11)

where

$$D_1 = 1$$

$$D_2 = 0.5948$$

$$D_3 = 1.9502(e/a)^2 + 0.7861(e/a) + 0.4812$$

$$D_4 = 3.1913(e/a)^4 + 1.6026(e/a)^3 + 1.8806(e/a)^2 + 0.4207(e/a) + 0.3963$$

$$D_5 = 6.8410(e/a)^6 + 3.6902(e/a)^5 + 2.7301(e/a)^4 + 1.4472(e/a)^3 + 1.8104(e/a)^2 + 0.3199(e/a) + 0.3354$$

$$D_6 = 0.303$$

The D_6 term in Eq. (A.11) was added to the approximate solution presented in $(\underline{A-9})$ to account for the incomplete series and allow M_m to become singular as the crack approaches the free surface. The value of M_m at Point Pt₂ is computed from Eq. (A.11) by substituting a negative value of e/a in the equations for the coefficients, and setting $D_6 = 0$.

<u>Sub-Surface Flaw in Bending (Point Pt₁)</u>

The curve fitting of the data for sub-surface flaws for bending was adequately handled using an incomplete cubic of two variables, 2e/t and 2a/t. Both angular positions on the crack front (i.e., points Pt_1 and Pt_2) were fit. These results for bending correction factor are given below.

$$M_{b} = E_{1} + \left[E_{2}(2e/t) + E_{3}(2e/t)^{2} + E_{4}(2e/t)(2a/t) + E_{5}(2a/t)(2e/t)^{2} + E_{6}(2a/t) + E_{7}(2a/t)^{2} + E_{8}(2e/t)(2a/t)^{2} + E_{9}\right] \left[\frac{1}{1 - (2e/t) - (2a/t)}\right]^{\frac{1}{2}} (A.12)$$

where

$$E_1 = 0.8408685$$
 $E_5 = 0.1294097$ $E_2 = 1.509002$ $E_6 = 0.8841685$ $E_3 = -0.603778$ $E_7 = -0.07410377$ $E_4 = -0.7731469$ $E_8 = 0.04428577$ $E_9 = -0.8338377$

for $0.1 \le 2a/t \le 0.7$ and $0 \le 2e/t \le 0.7$ as shown in Fig. 3.5.

Sub-Surface Flaw in Bending (Point Pt₂)

$$M_{b} = F_{1} + F_{2}(2e/t) + F_{3}(2e/t)^{2} + F_{4}(2e/t)(2a/t)$$

$$+ F_{5}(2a/t)(2e/t)^{2} + F_{6}(2a/t) + F_{7}(2a/t)^{2}$$

$$+ F_{8}(2e/t)(2a/t)^{2}$$
(A.13)

where

$$F_1 = -0.004378676$$
 $F_5 = 0.3805255$ $F_2 = 1.052083$ $F_6 = -0.44208$ $F_3 = -0.05479575$ $F_7 = -0.1208818$ $F_4 = -0.08603191$ $F_8 = 0.03725713$

for $0.1 \le 2a/t \le 0.7$ and $0 \le 2e/t \le 0.7$ as shown in Fig. 3.5.

A.4 ACCURACY OF EQUATIONS AND NUMERICAL RESULTS

The maximum numerical error in calculating Q using Eq. (A.5) was 0.23%. The maximum errors in the calculation of $M_{\rm m}$ and $M_{\rm b}$ from Eqs. (A.8) through (A.13) are typically less than 4% with average errors being approximately one-half the maximum level. These curve-fitting errors are based on the percentage differences between the equational values and the tabular data points used by the curve-fit program to formulate the expressions.

It should be noted that the maximum number of significant digits for $M_{\rm m}$ and $M_{\rm b}$ is three, since, at best, only three significant digits can be ascertained from the graphs. The eight digits shown in the coefficients of Eqs. (A.8) through (A.13) are presented only to indicate precisely the equations used in the function routines of FACET.